Review

Advances in Functional Vascular Stents for Cardiovascular Therapy with Drug Delivery and Computational Design

Xiaotian Xu [†], Qiang Liu [*,†], Yan Hu, Haifang Li, Yu Wang, Jiayi Sun, Kairong Qin

Posted Date: 8 June 2026

doi: 10.20944/preprints202606.0497.v1

Keywords: computer design; drug delivery; hemodynamic; vascular stents

 doi:10.20944/preprints202606.0497.v1

Review

Advances in Functional Vascular Stents for Cardiovascular Therapy with Drug Delivery and Computational Design

Xiaotian Xu [1,2,†], Qiang Liu [1,2,*,†], Yan Hu [3], Haifang Li [4], Yu Wang [2], Jiayi Sun [1,*] and Kairong Qin [2,*]

[1] Central Hospital of Dalian University of Technology, Dalian, 116089, P. R. China
[2] Faculty of Medicine, Dalian University of Technology, Dalian 116024, P. R. China
[3] School of Software Technology, Dalian University of Technology, Dalian 116024, P. R. China
[4] Department of AI and Informatics, Mayo Clinic, Jacksonville, Florida 32224, USA
* Correspondence: andyliu_1844@dlut.edu.cn (Q.L.); 12150004@qq.com (J.S.); krqin@dlut.edu.cn (K.Q.)
† These authors contributed equally to this work.

Abstract

Vascular stents are crucial devices in the treatment of cardiovascular diseases, and their structural design and function critically affect therapeutic efficacy and patient prognosis. Conventional stents can effectively restore vascular patency by providing mechanical support to blood vessels. However, they still face significant challenges including restenosis, thrombosis, and limited adaptability to complex patient-specific lesion characteristics. To address these limitations, drug delivery offers an important strategy to modulate the pathological microenvironment, enhance long-term vascular healing, and reduce systemic side effects. Meanwhile, advances in computational simulations have provided powerful tools for optimizing stent design through structural mechanics, hemodynamics, and drug release modeling, computational approaches enable the rational design of stent architectures with improved mechanical stability, vascular compatibility, and therapeutic regulation. Consequently, the development of vascular stents is evolving toward the synergistic integration of drug delivery, structural optimization, and intelligent design. This review summarizes the latest advances in functional vascular stents, clinical applications and computational design. This work aims to provide valuable insights for the engineering of efficient, precise, and intelligent vascular stents for cardiovascular therapies.

Keywords: computer design; drug delivery; hemodynamic; vascular stents

1. Introduction

Cardiovascular disease remains one of the leading causes of death and disability, with stenotic and structural abnormalities frequently involving the coronary arteries, peripheral arteries and aorta, all of which commonly require revascularization interventions. Among current therapeutic strategies. Percutaneous vascular intervention, particularly vascular stent implantation, is a key treatment for these diseases. Over decades of development, the materials and design of vascular stents have undergone several significant iterations, leading to continuous improvements in clinical efficacy. First-generation bare-metal stents (BMS) successfully addressed elastic recoil following balloon angioplasty alone, yet they were limited by high rates of in-stent restenosis (ISR) [1,2]. Subsequently, drug-eluting stents (DES) emerged as a major advancement which could significantly reduce ISR using antiproliferative drug coatings. However, the risk of late stent thrombosis (ST) remained a concern [3,4]. More recently, bioresorbable scaffolds (BRS) have been to developed to provide temporary mechanical support followed by gradual degradation, thereby mitigating the long-term risks associated with permanent metallic implants [5,6]. This progressive evolution of stent

 doi:10.20944/preprints202606.0497.v1

technology reflects a broader transition in biomaterials from non-degradable metals to biodegradable metals and polymers. Although these advances, conventional stents remain prone to post-implantation complications such as ISR and late thrombosis. To address these challenges, drug delivery has emerged as an important strategy in next-generation stent design [7,8]. By incorporating therapeutic agents, stents can regulate the local pathological microenvironment [9], extend the duration of therapeutic action [8] and lower systemic side effects [10], thereby significantly improving biological responses and long-term efficacy. To effectively implement these delivery functions, various carriers, including hydrogels, fibers, nanoparticles, and microspheres, have been incorporated into vascular stents. These carriers not only further mitigate adverse effects and enhance localized biological response but also provide a critical technological framework for the precision release of therapeutic agents [10,11]. For the design of drug delivery in vascular stents, computational simulation plays a key role to optimize vascular stents [12–15]. In the structural design phase, simulations can evaluate radial support, flexibility, and expansion uniformity of the stent, facilitating rational optimization of mechanical performance [16,17]. In hemodynamics analysis, simulations can model local blood flow changes after stent implantation [18]. Simulations can also clarify the relationship between these changes and restenosis [19]. In studies of therapeutic agent delivery, simulation approaches allow quantitative prediction of kinetic mechanisms of agent release from carriers [20]. They also show how agents transport through the vessel wall and bind to tissues [14,21]. Collectively, these computational strategies provide a powerful framework for integrating mechanical, hemodynamic, and biological considerations in stent development.

In recent years, the rapid development of artificial intelligence (AI) has provided new solutions for the application and research of vascular stent development, including stent material selection, carrier design, simulation optimization, and clinical decision-making. In this context, vascular stent technology is progressively evolving from mechanical implant toward an integrated therapeutic system that combinesstructural support of material, controlled drug delivery, intelligent design and potential clinical application (Figure 1) [22–24]. Therefore, this review summarizes current research landscape in functional vascular stents, with a focus on material innovation, drug delivery carriers, computational simulation, and emerging AI-driven approaches. This work aims to provide a perspective for the development of personalized, intelligent, and precision vascular stents.

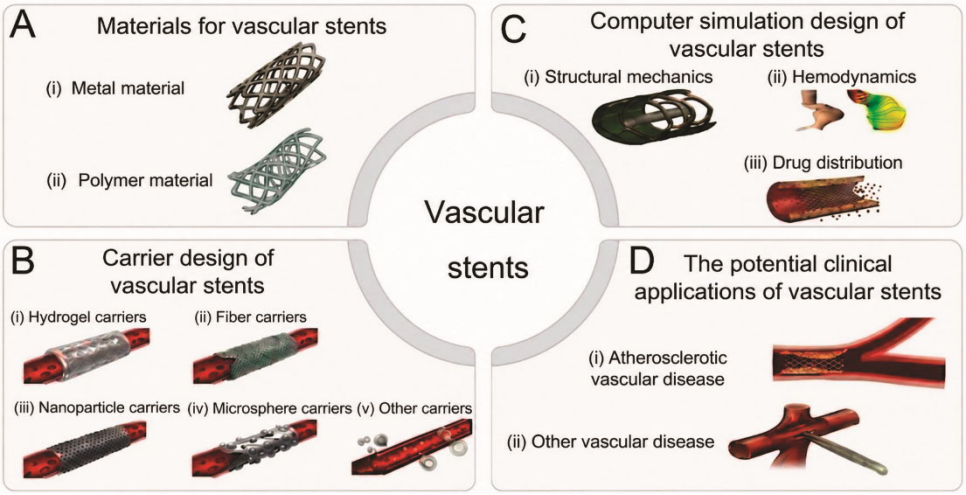

Figure 1. Summary of the full text logic [22–24].

2. Materials for Vascular Stents

The choice of stent materials plays an important role in determining the mechanical performance [25], biocompatibility [26], degradation behavior and long-term clinical outcomes [27]. To meet the evolving clinical demands for vascular intervention, several types of stent materials have been developed and optimization. Early non-degradable bare metal stents composed primarily of non-

 doi:10.20944/preprints202606.0497.v1

degradable metallic alloys, were designed to provide mechanical support to blood vessels [28]. However, concerns regarding long-term reactions, chronic inflammation, and the permanent presence of implants have driven the development of biodegradable metallic and polymeric stents, which offer improved biological adaptability and the potential for complete [29,30].

Based on their material composition, stents can be broadly categorized into metallic stents and polymeric stents, each possessing distinct advantages and limitations, while Table 1 provides an overview of their representative types, key properties, and current challenges.

Table 1. Classification, core characteristics and main limitations of vascular stent materials.

Material Classification	Representative Materials	Core Characteristics	Main Limitations
Non-degradable Metals	Stainless Steel	First stent material, excellent mechanical properties, low cost	High ISR rate, permanent retention
	Cobalt-chromium Alloy	High strength and radiopacity, allows for thin-strut stents	Risk of nickel ion allergy, permanent retention
	Platinum-chromium Alloy	Combines high strength and good radiopacity	Permanent retention
	Nickel-titanium Alloy (Nitinol)	Superelasticity, shape memory, self-expanding	Potential toxicity of nickel ions, permanent retention
Biodegradable Metals	Magnesium Alloy	First commercial biodegradable metal stent; mechanical properties superior to polymers	Degrades too fast, hydrogen gas production
	Iron Alloy	Excellent mechanical properties (close to stainless steel)	Degrades too slowly
	Zinc Alloy	Moderate degradation rate (between magnesium and iron)	Mechanical properties need improvement
Biodegradable Polymers	Polyesters	Fully degradable, tunable degradation rate (6 months to >2 years)	Insufficient radial support, lower mechanical properties than metals
	Polyurethanes	Smart responsiveness, excellent biocompatibility	Long-term stability remains to be verified
	Polycarbonates	Inherent X-ray opacity, radial strength superior to PLLA	Long degradation period (36-48 months)

2.1. Metallic Materials

Metallic materials were used in the early stage to fabricate vascular stents due to their excellent mechanical properties and good biocompatibility, and they continue to be widely used today [26,31]. With the advancement of manufacturing technologies, metallic stents can be classified into non-degradable and biodegradable metallic stents according to their degradability [2].

2.1.1. Non-Degradable Metals

Non-degradable metallic stents are the earliest class of vascular stents used in interventional therapy and remain widely applied today [32,33]. The initially developed devices were uncoated bare-metal stents [34]. These stents are primarily manufactured from stainless steel (SS), cobalt-chromium (Co-Cr), platinum-chromium (Pt-Cr), and Nitinol [34,35]. They offer distinct advantages, including robust mechanical strength, reliable radial support, and excellent biocompatibility at a low cost [34–36].Stainless steel served as the pioneering material for BMS. Its corrosion resistance and mechanical stability have facilitated its long-term clinical application [34,37]. However, the primary limitation of BMS is their permanent retention within the blood vessel. In-stent restenosis remains a

 doi:10.20944/preprints202606.0497.v1

major potential risk [38]. Stent implantation can disrupt the endothelialization process, thereby inducing abnormal smooth muscle cell proliferation and extracellular matrix deposition [39]. The resulting neointimal layer may lead to in-stent lumen re-narrowing. Furthermore, the rigid structure of metal stents may hinder natural vascular remodeling and endothelialization [34]. They also create a compliance mismatch with the native vessel. Over the long term, this mechanical caging may permanently impair the physiological vasomotor function of the vascular wall [40]. To address the issue of in-stent restenosis with bare metal stents, multiple studies have developed drug-eluting stents. DES utilize a non-degradable metallic framework coated with antiproliferative drugs [41]. This design significantly reduces the restenosis rate [1]. Additionally, stent grafts represent a critical application of metallic stents in aortic diseases. Stent grafts rely on a non-degradable metallic skeleton enveloped by a polymer membrane, and demonstrate good safety and efficacy [42]. Despite the significant clinical success of BMS, DES, and stent grafts, their fundamental characteristic remains unaltered. The non-degradable metallic framework permanently resides within the body. Consequently, these devices continue to face formidable challenges regarding long-term safety.

2.1.2. Degradable Metals

To overcome the long-term risks associated with the permanent presence of non-degradable metallic stents, degradable metallic stents have been developed. These devices aim to provide essential temporary mechanical support during vascular endothelial repair and tissue remodeling [26]. Subsequently, they progressively degrade and are absorbed by the body over months to years [43]. This temporary nature eliminates the complications caused by permanent implants [44]. Currently, magnesium (Mg) alloys are a primary focus of investigation in this field [26]. Some have achieved clinical translation and have degraded in vivo into highly biocompatible products [45,46]. Mg alloy stents provide reliable radial support during the initial implantation phase [47]. Recent clinical trials have also confirmed the robust clinical safety and efficacy of commercially available degradable Mg alloy stents [48–50]. Beyond Mg, researchers are actively exploring novel degradable metallic stents based on zinc (Zn) and iron (Fe) alloys. Zn alloys exhibit a degradation rate that is intermediate between those of Mg and Fe [51], which is often considered to be more compatible with the desired timescale for vascular remodeling [52,53]. At appropriate physiological concentrations, zinc ions can facilitate key cellular events that are prerequisite for endothelialization, such as the proliferation and migration of endothelial cells [54]. Conversely, Fe alloys offer excellent mechanical properties, with a radial strength comparable to stainless steel [16,51]. However, their clinical application is hindered by a slow degradation rate [51]. Collectively, these three degradable metals present distinct advantages and limitations, offering diverse options for the advanced design of next-generation degradable stents.

Metallic vascular stents are evolving from permanent implants to degradable platforms [44]. Correspondingly, stent materials have advanced from conventional stainless steel to bioresorbable metallic systems predominantly represented by Mg alloys [55,56]. Despite these advancements, current degradable metals still possess inherent limitations. Therefore, synergistically optimizing mechanical strength and degradation kinetics remains the core challenge for the future development of degradable metallic stents [51,57].

2.2. Polymer Materials

Materials science and medical engineering are becoming deeply integrated. Similar to metallic vascular stents, polymeric stents can be divided into two categories based on their degradation behavior, i.e., non-degradable and degradable. Degradable polymeric stents, made from PLLA, PLGA, PCL, PLCL and other polymers, offer unique degradability, biocompatibility, and design flexibility. As a result, they have gradually become a research hotspot in the field of vascular stents. However, non-degradable polymers have significant limitations in mechanical properties and long-term biostability [2]. Their clinical application is extremely rare. Therefore, most research efforts have shifted toward degradable polymeric vascular stents.

 doi:10.20944/preprints202606.0497.v1

Degradable polymeric vascular stents have achieved relatively broad clinical application, and related research has advanced considerably [29]. Their core advantage lies in complete degradation and absorption after fulfilling the mechanical support function, thereby avoiding the long-term risks associated with permanent implants and potentially restoring normal vascular vasomotion [5]. Based on chemical structure, degradable polymers can be mainly classified into polyesters (e.g., PLLA, PLGA, PCL), polyurethanes (e.g., zwitterionic polyurethane), and polycarbonates (e.g., tyrosine-derived polycarbonate) [2,58,59]. Polyesters are the most widely studied and applied biodegradable synthetic polymers, with PLLA as a representative example, constituting the main material of first-generation BRS [60]. However, first-generation BRS based on PLLA exhibited a relatively high risk of stent thrombosis in early clinical trials due to issues such as thick struts and insufficient radial strength [29,61]. To address these limitations, subsequent studies have improved polymer processing techniques (e.g., crystallization optimization) and developed copolymers (e.g., PLGA). Polyurethane materials have been introduced as novel smart polymers for stent design, such as zwitterionic polyurethane and poly (urethane-urea) elastomers, which exhibit excellent hemocompatibility and adaptive mechanical properties [62]. Studies have shown that with process optimization and material improvements, this class of vascular stents can achieve better clinical performance. Polycarbonate materials, represented by tyrosine-derived polycarbonates, have been investigated for vascular stent applications based on L-tyrosine pseudo-poly (amino acids) and other tyrosine analogues. These materials utilize natural amino acids as building blocks, allowing for tunable backbone structures through chemical synthesis. Their advantages include excellent biocompatibility, controllable degradation, and inherent radiopacity achieved via molecular design (e.g., iodinated tyrosine rings), which facilitates clinical imaging follow-up. The potential of such materials to improve radial strength and reduce strut thickness has been well-validated [2,63]. Meanwhile, the emergence of additive manufacturing (3D/4D printing) technologies has provided new possibilities for the design and fabrication of synthetic polymer stents. 3D printing facilitates the fabrication of stents with complex topological geometries to optimize mechanical characteristics while allowing for patient-specific customization, and such well-designed geometric configurations are capable of improving the local haemodynamic environment [46,64,65]. Furthermore, 4D printing has been explored to achieve a milder, more conformable self-expanding process, thereby reducing vascular wall injury caused by dilation [66]. Shape memory polymers have been confirmed as one of the key materials for 4D printing of vascular tissue-related constructs [67]. In addition to these synthetic polymers, natural polymers such as silk fibroin, collagen, and chitosan offer superior biocompatibility, low immunogenicity, and the capacity to promote cell adhesion and proliferation, making them attractive candidates for vascular repair [68–72]. These materials offer superior biocompatibility, low immunogenicity, and the capacity to promote cell adhesion and proliferation [68,70,73]. While less commonly used for stents, natural polymers have been extensively investigated for tissue-engineered vascular grafts (TEVGs) [74–76]. Researchers utilize techniques such as electrospinning, freeze-drying, and 3D bioprinting to fabricate grafts for the replacement of diseased vessels. These constructs eventually remodel into functional vascular tissues in vivo. Although these studies do not focus directly on stent design, they provide innovative strategies for vascular restoration.

In summary, this section outlined the evolution of stent materials from non-degradable metals to biodegradable metals and polymers. The following section shifts the focus to how carrier systems can complement these bulk materials by imparting additional therapeutic functions.

3. Carrier Design of the Vascular Stent

While contemporary bulk materials have made significant advancements in mechanical support and degradation control [2,26] , they alone are insufficient to meet the complex biological requirements of vascular repair [11,77]. These sophisticated demands include anti-proliferation [78], pro-endothelialization [79], anti-thrombosis [80], and temporal regulation [81]. Carrier systems can load and protect various therapeutic agents, control their release in a spatiotemporal manner, actively remodel the local pathological microenvironment, and promote endothelial cell proliferation [11,82].

 doi:10.20944/preprints202606.0497.v1

Therefore, the incorporation of carriers into stent systems can significantly expand their therapeutic functions. Figure 2 illustrates the microstructure and release kinetics of four typical stent-based carriers [78,83–85], accordingly, this section focuses on their design strategies.

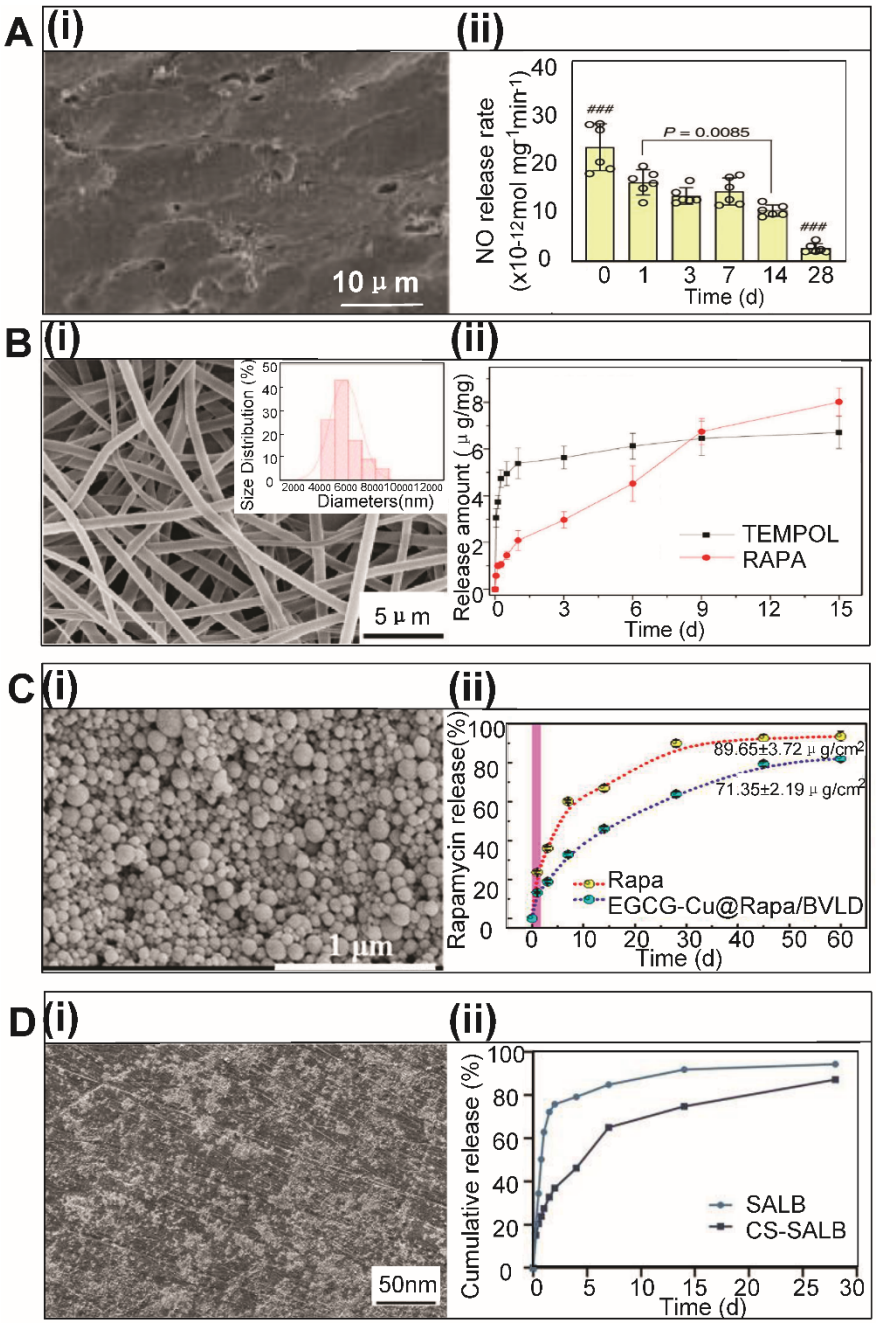

Figure 2. Microscopic morphologies and controlled release kinetics of four typical stent-based carriers. (A) Hydrogel: (i) Scanning electron microscopy (SEM) image of the NO-eluting hydrogel coating after in vitro balloon dilation. (ii) In vitro NO release over 28 days [83]. (B) Fiber: (i) SEM image of the electrospun nanofiber membrane co-loaded with rapamycin and TEMPOL. The inset shows the statistical histogram of the corresponding nanofiber diameter distribution. (ii) In vitro cumulative release of rapamycin and TEMPOL over 15 days [84]. (C) Nanoparticle: (i) SEM image of the drug-loaded nanoparticle composite coating with polyphenol-cross-linked network. (ii) In vitro cumulative release profile of rapamycin from the nanoparticle coating over 60 days [85]. (D) Microsphere: (i) SEM image showing the surface morphology of a nickel-titanium (NiTi) alloy functionalized with salvianolic acid B-loaded chitosan (CS-SALB) microspheres. (ii) In vitro salvianolic acid B release over 28 days [78].

 doi:10.20944/preprints202606.0497.v1

3.1. Hydrogel Carriers

Hydrogels possess unique three-dimensional hydrophilic networks, excellent biocompatibility, tunable degradation behavior, and mild drug-loading conditions, rendering them highly suitable for the functional modification of vascular stents [86]. Some studies suggest that hydrogels are unsuitable as bulk materials for vascular stents due to their insufficient mechanical strength and inability to maintain luminal patency [87]. Although recent studies have preliminarily validated the feasibility of hydrogels as bulk vascular implants [88], to our knowledge, structural hydrogel carriers remain at the stage of proof of concept. In contrast, functional hydrogel carriers have made substantial progress, presenting a clearer path toward clinical translation. The core mission of these carriers is to endow stents with active delivery capabilities. Acting as reservoirs for bioactive molecules, they enable the precise delivery of therapeutic agents to target sites and facilitate local intervention through hydrogel swelling, diffusion, or degradation [89–91]. Furthermore, hydrogel carriers enable targeted drug delivery. One study used thermosensitive Pluronic F-127 hydrogel as a rapamycin carrier. By tuning the porosity of porous NiTi alloy (0%–40%), it achieved precise control over drug loading and sustained release for up to 17 days, effectively inhibiting smooth muscle cell (SMC) proliferation [92]. Building on this, another study developed a bilayer coating composed of rapamycin-loaded PLGA and heparin-loaded alginate hydrogel. The coating enabled the release of both agents from the stent surface, achieving synergistic anti-proliferative and anticoagulant effects [93]. In addition, an asymmetric coating strategy was employed: a heparin-loaded alginate hydrogel coating and an atorvastatin calcium-loaded polyurethane electrospun fiber coating were fabricated on coronary stents. This dual-drug release design provided multimodal therapeutic benefits [94]. These advances demonstrate that hydrogel drug delivery systems are evolving from single-agent release toward multi-drug synergy and spatial control. Hydrogel carriers also support growth factor delivery. One study encapsulated human vascular endothelial growth factor-165 ($VEGF_{165}$) in calcium alginate microspheres, which were then dispersed with paclitaxel-loaded micelles in a polyvinyl alcohol (PVA) hydrogel matrix. This system achieved rapid short-term VEGF release to promote early endothelialization, while sustained long-term paclitaxel release inhibited late SMC proliferation. This combinatorial delivery approach may better match the stage-specific therapeutic requirements of vascular injury repair [95]. Hydrogel carriers are capable of gene delivery as well. Cationized gelatin hydrogels have been shown to effectively deliver LacZ plasmid DNA and achieve sustained in vivo gene expression, confirming the fundamental feasibility of hydrogel-mediated non-viral gene delivery [96]. Subsequently, a cationized pullulan hydrogel delivered siRNA targeting matrix metalloproteinase 2 (MMP-2), resulting in reduced pro-MMP-2 activity [97]. Further work constructed a fibrin hydrogel gene reservoir via LbL self-assembly, which loaded and protected VEGF/Ang1 gene nanoparticles. In vivo experiments confirmed that this strategy significantly enhanced re-endothelialization [98]. These developments illustrate the progression of hydrogel gene delivery systems from proof-of-concept to therapeutic application. Additionally, hydrogel carriers enable gaseous molecule delivery. One study developed a mechanically robust nitric oxide (NO)-eluting hydrogel coating (Figure 2A) [83], which continuously generated NO by catalyzing endogenous substrates. In both rabbit and porcine stent models, this coating effectively suppressed local inflammation, accelerated re-endothelialization, and attenuated neointimal hyperplasia [83]. Furthermore, a hydrogel coating with sequential H_2S/NO release was fabricated: an early H_2S burst synergized with NO to inhibit thrombosis and inflammation, while sustained NO release maintained vascular homeostasis, leading to superior endothelialization and reduced intimal hyperplasia [99]. Additional gas delivery strategies have also been reported: a catechol-chitosan hydrogel coating loaded with Cu^{2+} catalyzed endogenous NO production [100], and a catechol-hyaluronic acid-cystamine hydrogel coating loaded with allicin (an H_2S donor) achieved oxidative stress-responsive on-demand release [101]. These examples highlight the tremendous potential of hydrogels in gas therapy for cardiovascular applications.

3.2. Fiber Carriers

 doi:10.20944/preprints202606.0497.v1

Fiber materials are widely employed as carriers for vascular stents due to their high specific surface area, high porosity, and fibrous network that effectively mimics the natural extracellular matrix [102]. Furthermore, these materials offer considerable flexibility in tailoring mechanical properties and degradation kinetics through material selection and fabrication process design [103,104]. Structural fiber carriers make use of fibers to directly form the stent body, maintaining luminal patency through their inherent mechanical properties [105]. While these polymeric materials, including PLLA, PCL, and PVA, were introduced from a material science perspective in Section 2.2, this section focuses specifically on their application as the primary structural components of stents. Beyond their role as functional coatings, structural fibers can also be engineered into the stent architecture itself. For instance, Lin et al. demonstrated the benefits of this approach by weaving PCL/PEG-coated PVA yarns into a vascular stent, followed by heat treatment to create a distinct skin–core structure. By exploiting the inherent designability of woven architectures, this approach endowed the stent with superior flexibility and elasticity, effectively demonstrating the structural advantages of utilizing fiber-based carriers as the stent body [106].

Functional fiber carriers endow stents with therapeutic functions, such as targeted drug delivery and biological activity regulation. Drug delivery via fiber carriers has been extensively investigated. For example, an asymmetric coating technique was adopted to fabricate a heparin-loaded alginate layer and an atorvastatin calcium-loaded polyurethane electrospun fiber layer on coronary stents, achieving dual-drug release [94]. Another study prepared paclitaxel-loaded PCL electrospun coatings for stents and systematically investigated the influence of coating deformation during stent expansion on drug release behavior. The results revealed that coating elongation did not induce fiber fracture, and drug release kinetics remained stable. This provides an important reference for the coating design of drug-eluting stents, demonstrating the stability and controllability of fiber carriers in drug delivery [107]. To achieve multi-dimensional interventions in complex pathological microenvironments, an electrospun nanofiber-covered stent co-loaded with rapamycin and the antioxidant TEMPOL was developed (Figure 2B). The fiber carrier achieved sustained and steady co-release of both therapeutics for up to 28 days. It inhibited smooth muscle cell proliferation while effectively scavenging local reactive oxygen species (ROS), thereby significantly promoting re-endothelialization and alleviating local inflammation [84]. Beyond drug delivery, fiber carriers have also been engineered to co-deliver drugs and growth factors for vascular stent applications. For instance, a PLCL nanofiber-covered stent co-loaded with heparin and VEGF was constructed to enable sustained dual release for 30 days, facilitating endothelial cell proliferation and stent re-endothelialization [108]. Advancing this approach, another study designed PLA electrospun fiber-covered stents with spatially compartmentalized delivery: VEGF was covalently immobilized on the fiber surface, while paclitaxel was encapsulated into mesoporous silica nanoparticles embedded within the fiber matrix. This architecture enabled the rapid release of VEGF alongside the long-term sustained release of paclitaxel, achieving spatiotemporal regulation of dual-agent release [109]. These advances indicate that growth factor delivery via fiber carriers is evolving toward sophisticated drug-factor combinations with spatiotemporally regulated release profiles.

3.3. Nanoparticle Carriers

Nanoparticles have been extensively utilized in vascular disease research and serve as highly effective carriers for vascular stents. This widespread application is driven by their unique advantages, including nanoscale size effects, high specific surface area, tunable surface chemistry, and remarkable capabilities for subcellular delivery and active targeting [110,111]. Currently, research on nanoparticles in the context of vascular stents predominantly focuses on their application as functional carriers. In this paradigm, the stent serves as a delivery platform loaded with nanoparticles to achieve therapeutic functions such as gene therapy, targeted drug delivery, and the inhibition of restenosis [112–114]. Nanoparticles have a wide range of applications in vascular stent technology, most notably in drug delivery. One study employed cationic electrodeposition to coat stent surfaces with bioabsorbable polymeric nanoparticles encapsulating a fluorescent marker. In a

 doi:10.20944/preprints202606.0497.v1

porcine coronary artery model, the resulting nanoparticle-eluting stent demonstrated sustained local drug release for up to 4 weeks without aggravating stent-induced inflammatory responses or neointimal hyperplasia [115]. Another study encapsulated sirolimus into nanoparticles and delivered them locally to the stent implantation site, confirming their inhibitory effect on in-stent restenosis in a preclinical model [116]. Similarly, pitavastatin-loaded nanoparticle-eluting vascular stents effectively inhibited in-stent restenosis without delaying endothelial healing in a porcine coronary artery model, offering new insights into overcoming the side effects of conventional drug-eluting stents [117]. Beyond the choice of therapeutic agents, the structural design of nanoparticle coatings critically influences stent performance. To improve coating stability and controlled release performance, one study constructed a polyphenol-metal cross-linking network formed by copper ions and epigallocatechin gallate (EGCG) on the stent surface. This network self-assembled into a nanoparticle-embedded structure that directly encapsulated rapamycin (as shown in Figure 2C). This composite coating achieved sustained drug release for up to 60 days, demonstrating excellent dual efficacy in modulating inflammation and promoting vascular healing [85]. To further improve delivery efficiency, researchers have introduced targeting strategies. Chorny et al. applied magnetic targeting by encapsulating paclitaxel into magnetic nanoparticles, which, under an external uniform magnetic field, facilitated localized accumulation at the stent and significantly enhanced drug retention at the injury site [118]. They subsequently reviewed the promise of magnetic nanoparticles for targeted vascular delivery and discussed the potential of uniform magnetic field-mediated targeting strategies in preventing in-stent restenosis [114]. Furthermore, Zhao et al. constructed reactive oxygen species (ROS)-responsive nanoclusters loaded with RVX-208. Following intravenous injection, these clusters specifically dissociate and release the drug under the high-ROS environment of the arterial injury site, achieving an “on-demand” release profile that minimizes systemic exposure while enhancing local therapeutic efficacy [119]. Nanoparticles also enable highly effective gene delivery. Che et al. complexed Akt1 siRNA with disulfide-crosslinked low-molecular-weight polyethylenimine to form nanoparticles, which were applied onto a hyaluronic acid-coated stent surface. In vivo experiments in a rabbit model demonstrated that this approach significantly inhibited smooth muscle cell growth [112]. Building on this, the same team systematically investigated the therapeutic effect of this Akt1 siRNA nanoparticle-eluting stent on restenosis following balloon injury, further confirming the feasibility of the strategy through micro-CT and histological analyses [120]. The same group also loaded miR-145 into the identical carrier system, validating its inhibitory effect on restenosis in a rabbit iliac artery stent model [113]. Moreover, Izuhara et al. developed a miR-126-loaded nanoparticle-eluting vascular stent, demonstrating its significant suppression of neointimal formation in a rabbit model [121]. Another study utilized ultrasound-mediated magnetic nanoparticle delivery of Pik3cb shRNA and confirmed its inhibitory effect on intimal thickening in a rat balloon injury model [122]. Collectively, these studies indicate that nanoparticle-mediated gene delivery is advancing from siRNA to miRNA, from single to multiple targets, and from passive release to physical field-assisted delivery. Apart from gene delivery, nanoparticles also enable gasotransmitter delivery to achieve multifunctional stent coatings. Luo et al. constructed a surface coating loaded with heparin nanoparticles that simultaneously generates NO, achieving dual anticoagulant and pro-endothelialization functions [123]. The application of nanoparticle carriers in vascular stents has also extended to emerging areas such as immunomodulation. Li et al. developed a rapamycin-loaded, platelet membrane-camouflaged biomimetic nanoparticle-coated stent, which promoted vascular healing by modulating the cGMP-PKG and NF-κB signaling pathways [124]. Hou et al. immobilized exosomes onto the surface of biodegradable magnesium alloy stents, harnessing the natural bioactive molecules within exosomes to achieve anti-inflammatory and pro-endothelialization functions [125]. Polyak et al. employed magnetically mediated targeted delivery of superparamagnetic nanoparticle-loaded endothelial cells, demonstrating significant inhibition of in-stent stenosis in a rat carotid artery stent model [126]. These emerging strategies expand the application boundaries of nanoparticles in vascular stents and open up new possibilities for functionalized design.

 doi:10.20944/preprints202606.0497.v1

3.4. Microsphere Carriers

Microspheres serve as highly effective carriers for vascular stents due to their core advantages, including tunable size and architecture, high drug-loading capacity, and programmable release kinetics [127–129]. Also acting as functional carriers, they are primarily utilized to achieve the localized and controlled release of therapeutic agents [130,131].

One primary application of microsphere carriers is drug delivery. One study embedded PLGA microspheres loaded with hydrophilic drugs into a hydrogel coating, tailoring the drug release rate by altering the polymer formulation [128]. Another study assembled silk fibroin microspheres loaded with both paclitaxel and metformin onto the surface of a woven stent-graft via electrostatic bonding. This dual-drug synergy achieved robust anti-proliferative functions, with in vitro release sustained for over 70 hours [129]. Furthermore, researchers constructed salvianolic acid B-loaded chitosan microspheres on a nitinol vascular stent utilizing a dopamine-mediated strategy (as shown in Figure 2D). Leveraging the dual bioactivity of salvianolic acid B, this microsphere structure significantly inhibited the proliferation and migration of smooth muscle cells in vitro while promoting the adhesion and proliferation of endothelial cells, offering a reliable strategy for the long-term prevention of in-stent restenosis [78]. To enhance anticoagulant function, another study immobilized heparin/poly-L-lysine microspheres onto a dopamine-coated stent surface. This approach significantly prolonged both the activated partial thromboplastin time (APTT) and thrombin time (TT), demonstrating excellent anticoagulant activity alongside promoted endothelial cell adhesion and proliferation [131]. Collectively, these studies indicate that microsphere-mediated drug delivery is evolving from single-agent formulations to dual-drug synergy, and from mono-functional to multi-functional designs. Beyond traditional pharmacotherapeutics, microspheres also facilitate the localized delivery of bioactive factors. For instance, biodegradable microspheres encapsulating NO donors have been incorporated into vascular stents. These stents achieved an initial NO burst release during the first week followed by sustained release for three weeks, significantly reducing the intima-to-media ratio by 46% and 32% at 7 and 28 days post-implantation, respectively [130]. In another study, a composite coating consisting of basic fibroblast growth factor (bFGF)-loaded gelatin hydrogels and argatroban-loaded PLGA microspheres was applied to cerebral aneurysm stents. This configuration promoted connective tissue formation within the aneurysm cavity while reducing the incidence of in-stent thrombosis [127]. This highlights that microsphere-based factor delivery is expanding from small-molecule gas therapeutics to protein-based biologics, and enables the construction of multi-agent composite coatings. Microspheres also enable advanced cell-loading strategies. One study utilized superparamagnetic iron oxide microspheres to intracellularly label endothelial cells. Through the magnetic forces generated by a magnetized stent, these cells were successfully captured and retained at the implantation site, providing a novel paradigm for accelerating stent surface endothelialization [132]. Additionally, microspheres can function directly as embolic agents. In aneurysm treatment, a recent strategy involves deploying a flow-diverting stent followed by the injection of 500–900 μm microspheres into the aneurysm sac through the stent interstices. Acting as a mechanical barrier to prevent microsphere migration, the stent facilitates safe and complete aneurysm occlusion [133]. This innovative approach broadens the role of microspheres in vascular stent-related therapies, extending their application from therapeutic delivery to interventional embolization.

3.5. Other Carriers

Beyond the aforementioned hydrogels, fibers, nanoparticles, and microspheres, a variety of novel carrier systems have emerged in recent years, further enriching the functional design strategies for vascular stents. Research on the application of functional carriers (e.g., liposomes, exosomes, and viral vectors) is continuously advancing, offering novel solutions for localized drug and gene delivery.

Liposomes, vesicular structures composed of phospholipid bilayers, have garnered widespread attention in vascular stent drug delivery systems due to their excellent biocompatibility, capacity to

 doi:10.20944/preprints202606.0497.v1

encapsulate both hydrophilic and hydrophobic drugs, and amenability to functional modification. In the realm of drug delivery, alendronate-loaded liposomes exert anti-inflammatory effects by specifically targeting monocytes and macrophages; systemic administration of these liposomes significantly inhibits neointimal hyperplasia following stent implantation [134]. Furthermore, while sirolimus is a conventionally utilized anti-proliferative agent in drug-eluting stents, its clinical efficacy is often hindered by poor aqueous solubility and low bioavailability. Nanocarriers such as liposomes can effectively overcome these limitations to enhance its delivery efficiency [135]. In the field of gene delivery, complexes formed by cationic liposomes and nucleic acids within vascular stents enable the localized gene transfection of vascular tissues [136]. Specifically, liposome-functionalized stents carrying the endothelial nitric oxide synthase (eNOS) gene have been demonstrated to accelerate re-endothelialization [137]. Expanding into gasotransmitter delivery, stent nanocoatings integrating NO-releasing peptide amphiphiles with liposome-encapsulated anti-proliferative agents can exert potent synergistic therapeutic effects [138].

Exosome carriers are nanoscale vesicles (30–150 nm) secreted by cells, carrying a variety of bioactive molecules such as proteins, mRNA, and miRNA, and possessing natural intercellular communication functions [139]. In the field of gene delivery, one study loaded plant-derived exosome-like nanoparticles with CA1-siRNA and achieved targeted delivery to aortic injury sites, effectively inhibiting in-stent restenosis [140]. Furthermore, as discussed in Section 3.3, exosomes themselves can also serve as therapeutic agents. Another study developed a mesenchymal stem cell-derived exosome-eluting vascular stent that releases exosomes locally to promote endothelial cell proliferation, inhibit smooth muscle cell migration, and improve vascular healing [141].

Viral carriers hold significant value in the field of vascular stent gene therapy owing to their high gene transduction efficiency. In the context of gene delivery, one study covalently anchored Protein G to the metallic stent surface, utilizing its natural binding affinity for the Fc region of mammalian IgG to capture adeno-associated virus, thereby enabling vector-mediated gene delivery from the vascular stent [142]. Building on this affinity-based strategy, another study reversibly anchored adenoviral or adeno-associated viral vectors directly onto metallic stent surfaces via hydrolyzable crosslinkers, achieving localized and controlled gene delivery [143]. Furthermore, viral vectors can also be delivered within vascular stents using a balloon catheter; one study employed this approach to achieve local intraluminal delivery of adenoviral VEGF-A at the stent site, significantly accelerating the re-endothelialization process on the stent surface [144].

In summary, the diverse carrier systems discussed have advanced vascular stents from passive mechanical scaffolds to intelligent systems that actively modulate the vascular repair microenvironment. However, their full therapeutic potential requires precise optimization of carrier distribution, release kinetics, and local biomechanical interactions. Computational simulation technologies provide a systematic framework to address these challenges.

4. Computational Design of Vascular Stents

Computational simulation studies of vascular stents use computer modeling techniques to analyze stent mechanical performance, hemodynamic effects, interactions between stents and blood vessels, and therapeutic agent transport and delivery in a virtual environment, providing critical evidence for design optimization and preclinical evaluation. Figure 3 illustrates representative simulation approaches for vascular stents across three core perspectives: structural mechanics simulation [145], hemodynamic simulation [146], and drug release and distribution simulation [14]. These computational techniques can intuitively predict the structural and mechanical responses of stents, local vascular hemodynamic changes, and targeted drug release and delivery behaviors under different stent and carrier configurations. They ultimately guide the synergistic optimization of integrated stent and carrier systems. Such computational design approaches provide a theoretical foundation for developing advanced clinical vascular stents and their personalized applications.

 doi:10.20944/preprints202606.0497.v1

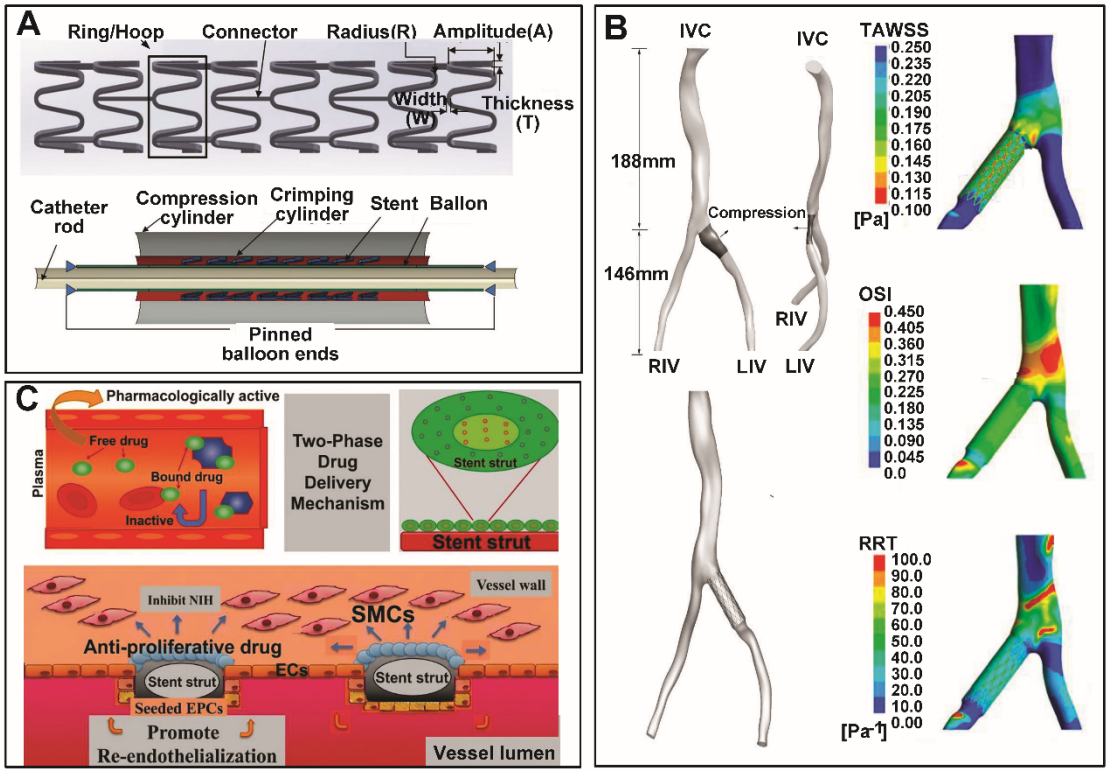

Figure 3. Multiphysics computational simulations for vascular stents. (A) Stent geometric parameters and multibody finite element analysis framework. Open-cell stent design parameters for structural optimization and a full-scale model predicting stent crimping and expansion behaviors are shown [145]. (B) Iliac vein hemodynamic simulations. Native and post-stenting iliac vein models are presented alongside the distributions of time-averaged wall shear stress, oscillatory shear index, and relative residence time, indicating the risks of neointimal hyperplasia and thrombosis [146]. (C) Drug-eluting stent two-phase drug delivery mechanisms. Free/bound drug equilibrium, polymer coating release kinetics, and the microenvironment of half-embedded struts are illustrated, demonstrating the drug targeting of smooth muscle cells and the promotion of endothelial repair [14].

4.1. Structural Mechanics Simulation of Vascular Stents

Structural mechanics simulation employs the finite element method (FEM) to analyze the mechanical behavior of vascular stents, providing a robust theoretical foundation for stent structural optimization.

4.1.1. Evaluation of Stent Mechanical Performance

Structural mechanics simulation is primarily based on finite element analysis (FEA) to quantitatively evaluate the key mechanical performance indicators of stents. The core quantifiable metrics include radial strength, elastic recoil, longitudinal foreshortening, dogboning, and bending flexibility. Radial strength, defined as the maximum external radial force a stent can withstand before collapse, is the most critical mechanical property for maintaining long-term luminal patency [24,147]. Elastic recoil and longitudinal foreshortening characterize the geometric stability of a stent after balloon deflation [147]. Excessive recoil leads to insufficient lumen gain, while significant foreshortening may result in incomplete lesion coverage or stent migration [148,149]. Dogboning refers to the non-uniform expansion phenomenon where the stent ends expand earlier and to a larger diameter than the central segment [150]. Severe dogboning can cause localized vascular wall injury [151] and insufficient stent deployment with increased residual stenosis [152]. Bending flexibility reflects the ability of a stent to navigate through tortuous blood vessels [24,153], which is essential for successful delivery and accurate deployment in complex anatomical configurations [154].

 doi:10.20944/preprints202606.0497.v1

Computational simulations enable accurate prediction and systematic evaluation of these mechanical metrics prior to prototype fabrication. This predictive capability significantly accelerates the stent development process, reduces experimental costs, and provides scientific guidance for the structural optimization of vascular stents.

4.1.2. Stent Structural Design and Parameter Optimization

Optimizing mechanical performance through structural design is a central application of simulation-based research. Finite element analysis (FEA) allows the rapid evaluation of different design concepts without extensive physical prototyping, significantly shortening the development cycle and reducing costs [155,156]. Targeting the key mechanical metrics discussed above, systematic stent design studies have been conducted with various optimization objectives. As illustrated in Figure 3A, parametric simulation enables the systematic investigation of how core geometric parameters, including crown amplitude (A), crown radius (R), strut width (W), and strut thickness (T), influence quantifiable mechanical performance indicators, thereby establishing quantitative relationships between design variables and mechanical responses [145]. Enhancing radial strength is one of the primary goals of structural optimization. Parametric finite element analysis can be employed to systematically examine the influence of support-ring geometry on radial strength. For example, the M-shaped bistable stent structure proposed by Xia et al., validated through simulation, overcomes the inherent limitations of conventional polymer stents, which rely on elastoplastic deformation, achieving a breakthrough improvement in radial strength [157]. The optimization of elastic recoil and longitudinal foreshortening aims to improve the geometric stability of stents after deployment. One study simulated the entire stent expansion process and found that an unequal-height support-ring design increased radial strength by more than 30% while significantly reducing elastic recoil [158]. Another study employed an optimization method integrating a Kriging surrogate model with finite element analysis, achieving a 66% reduction in recoil and a 60% reduction in foreshortening [159]. Furthermore, auxetic structures with a negative Poisson's ratio can effectively suppress foreshortening, with an optimized stent attaining a foreshortening ratio as low as 3.27% [160]. Mitigating the dog-boning effect seeks to enhance the uniformity of stent expansion. Simulation studies have shown that dog-boning can be effectively suppressed by optimizing the end-ring geometry or connector design, thereby reducing the associated risk of vascular injury [161] as well as by adjusting the balloon length [162]. Optimizing bending flexibility requires a careful balance between radial strength and conformability. Finite element models can accurately capture the deformation response of a stent in curved vessels, guiding the rational design of connectors and the configuration of support rings. This allows for substantial improvements in bending flexibility without compromising radial strength; in one study, the bending stiffness of the optimized stent was reduced by over 30%, leading to markedly enhanced deliverability and vascular wall apposition in tortuous vasculature [161].

In summary, structural mechanics simulation has become integral to all core stages of vascular stent design. It provides a systematic reference framework for stent development, ranging from the quantitative evaluation of key mechanical performance indicators to structural parameter optimization for specific objectives. Building on the material evolution discussed in Section 2, simulation analysis can further guide the matching optimization of different materials, including cobalt-chromium alloys, magnesium alloys, and PLLA, with appropriate structural designs. For example, simulations can predict the radial support performance of high-modulus materials with thin struts, or inform the design of optimized compensatory structures for low-modulus polymers. As simulation accuracy continues to improve and multiphysics coupling methods mature, structural mechanics simulation will play an increasingly critical role in the personalized design and preclinical evaluation of vascular stents.

4.2. Hemodynamic Simulation of Vascular Stents

 doi:10.20944/preprints202606.0497.v1

Vascular stent implantation disrupts native blood flow patterns, which is closely associated with post-procedural restenosis. Hemodynamic simulations enable quantitative assessment of these flow disturbances to guide stent design and clinical decision-making.

4.2.1. Evaluation of Hemodynamics

Hemodynamic simulations primarily relies on computational fluid dynamics (CFD) methods. It quantitatively evaluates hemodynamic parameters following stent implantation [163]. Wall shear stress (WSS), oscillatory shear index (OSI), and relative residence time (RRT) serve as key hemodynamic evaluation metrics for stents. Typical simulation setups and their corresponding results are illustrated in Figure 4B [146].

Wall shear stress represents the hemodynamic frictional force exerted by blood flow on the vascular endothelium, serving as a critical mechanical stimulus that mediates endothelial homeostasis [164]. Studies indicate that low WSS regions are closely associated with endothelial dysfunction [164], intimal hyperplasia [165], and restenosis [166]. A value of 0.5 Pa is commonly used as the reference threshold for identifying low WSS in research [167]. Time-averaged wall shear stress (TAWSS) can be calculated by temporally averaging the instantaneous WSS over a cardiac cycle. This metric is used to evaluate the average mechanical stimulation exerted by blood flow on the vascular wall [168]. The oscillatory shear index evaluates the oscillatory characteristics of blood flow throughout the cardiac cycle. It is an important hemodynamic metric for identifying flow disturbances and predicting the risk of in-stent restenosis [169]. Studies have shown that an abnormal elevation in OSI is closely related to local blood flow disturbances following stent implantation [170]. Relative residence time integrates information from both low TAWSS and high OSI [171]. It is a critical parameter for assessing the risk of in-stent restenosis [172]. An elevated RRT value reflects an abnormal local blood flow state and correlates with near-wall flow stagnation zones [173]. This stagnant state may lead to excessive uptake of inflammatory markers by the vascular wall [174]. Furthermore, it can promote platelet aggregation and adhesion, thereby increasing the risk of thrombosis [175]. Through the comprehensive analysis of these metrics, hemodynamic simulations can predict a stent's impact on the local blood flow environment prior to implantation. This capability provides a crucial theoretical basis for stent design optimization and preclinical evaluation.

4.2.2. Stent Design and Hemodynamic Optimization

The geometric design parameters of a stent, including strut thickness, cross-sectional shape, link configuration, and deployed state, significantly influence the post-implantation local hemodynamic environment [163,170]. Hemodynamic simulations enable a systematic evaluation of the impact of various design parameters on critical metrics such as wall shear stress, oscillatory shear index, and relative residence time. This evaluation provides a scientific foundation for the structural optimization of vascular stents. Regarding WSS, simulation studies demonstrate that strut cross-sectional shape, cell configuration, porosity, thickness, spacing, link design, and the deployed state significantly influence its distribution [176–178]. A teardrop-shaped streamlined cross-section can result in up to 96% of the inter-strut region maintaining a WSS above the critical threshold for in-stent restenosis (Mejia et al., 2009). In contrast, closed-cell stents exhibit larger areas of low WSS due to a greater number of struts protruding into the lumen [179], and lower porosity can further lead to a decrease in WSS [180]. While thicker struts can reduce the expansion of low WSS regions [181], narrower strut spacing tends to increase the area of adverse low WSS [176]. Additionally, link length and its alignment angle relative to the main flow are key factors affecting WSS distribution [170]. Furthermore, factors such as malapposition, increased strut protrusion [176], and overlapping can all lead to localized hemodynamic abnormalities [172]. Regarding OSI, simulation studies indicate that strut geometry, cell configuration, porosity, link design, and the deployed state significantly impact its distribution. Stents with rounded, low-profile struts exhibit the lowest proportion of high OSI (>0.2) regions [65]. On the other hand, design features that amplify flow disturbance, such as the increased strut number in closed-cell configurations [179] and higher porosity [180], as well as

 doi:10.20944/preprints202606.0497.v1

connector designs with suboptimal length or alignment angle [170], all contribute to elevated OSI. Beyond the baseline design, the deployed state can further elevate local OSI in cases of malapposition or overlapping, with the adverse effect of strut size being especially amplified in overlapping configurations [172]. As a metric integrating WSS and OSI information, the distribution of RRT is notably influenced by cell configuration, strut thickness, porosity, and the deployed state. Strut thickness has been identified as the design parameter most strongly correlated with RRT [182]. The area of elevated RRT is expanded in closed-cell stents [179]. Moreover, high-porosity designs can result in elevated RRT (Nada et al., 2021), and overlapping regions are particularly prone to RRT elevation [183].

In conclusion, stent design parameters profoundly affect local hemodynamics in multiple dimensions. Optimizing these geometric parameters can substantially reduce adverse flow zones with low WSS, high OSI, and elevated RRT. Improving the local hemodynamic microenvironment ultimately lowers the risk of in-stent restenosis and thrombosis. Hemodynamic simulations provide vital technical support for this multi-objective optimization.

4.3. Drug Distribution Simulation for Vascular Stents

Vascular stents can serve as carriers for a diverse array of therapeutic agents, including small-molecule drugs, growth factors, genes, and gas molecules. By establishing mathematical models of mass transport, current simulation studies on therapeutic delivery seek to elucidate the kinetic mechanisms that govern the release of these agents from their carriers, their subsequent transport within the vascular wall, and their eventual binding to local tissues.

4.3.1. Simulation of Drug Release, Transport and Target Binding

The mechanisms governing drug release from carriers are primarily categorized into three types: diffusion-controlled, degradation-controlled, and stimuli-responsive release [184]. Diffusion-controlled release is the most fundamental mode, where agent release is driven by concentration gradients in accordance with Fickian diffusion laws. Raval et al. mathematically modeled the release behavior of sirolimus from PLCL/PVP coatings, demonstrating that the process is jointly governed by surface dissolution and diffusion [185]. Zhao et al. employed a cylindrical diffusion model to quantitatively describe the everolimus release profiles from stent coatings. Their simulations revealed that a higher diffusion coefficient accelerates release, while increased coating thickness retards it. Furthermore, the in vitro diffusion coefficient was significantly higher than its in vivo counterpart, and the model-fitted thickness closely matched actual manufacturing specifications [186]. McGinty et al. investigated drug release mechanisms via analytical solutions, establishing multiple models, including pure diffusion and coupled dissolution-diffusion models. These formulations provide essential theoretical tools for estimating diffusion coefficients, dissolution rate constants, and tissue transport parameters from experimental data [187]. Degradation-controlled release involves the hydrolysis, erosion, or enzymatic degradation of the polymer matrix, with the drug release rate tightly coupled to the carrier's degradation kinetics. Formaggia et al. pioneered a comprehensive model incorporating drug dissolution, diffusion, and surface erosion. They revealed that the relative magnitude of dissolution and diffusion rates dictates the release mode: rapid dissolution forms a moving dissolution front, whereas rapid diffusion leads to a uniform depletion of the solid phase. Additionally, surface erosion was shown to accelerate release. Based on mass conservation principles, this model also derived coupling conditions at the interface between the coating and the tissue, ensuring strict mass conservation during drug transport between the two domains [188]. Zhu and Braatz further developed a coupled mathematical model integrating PLGA coating degradation, erosion, and drug release. Their model quantified how decreasing molecular weight and increasing porosity co-regulate release behavior. Specifically, a reduction in molecular weight leads to a power-law increase in the drug diffusion coefficient within the solid polymer phase, while increased porosity creates liquid-phase diffusion pathways; together, these mechanisms synergistically modulate the release rate [189]. Additionally, Naghipoor et al. developed a non-Fickian mass transport model to

 doi:10.20944/preprints202606.0497.v1

systematically analyze the effects of polymer porosity and degradation rate. Their results indicated that a higher degradation rate yields a lower peak drug concentration. When time-dependent porosity was accounted for, the drug exited the stent more rapidly but exhibited a shorter residence time within the vascular wall. Conversely, a higher dissolution rate produced a higher peak concentration but a faster subsequent decay [190]. Stimuli-responsive release refers to systems where the carrier responds to physiological signals, such as pH, temperature, enzymes, or reactive oxygen species, to achieve on-demand delivery of therapeutic agents. Furthermore, utilizing finite element methods, Gagliardi analyzed the drug concentration distributions across three commercial stents, demonstrating that stent geometric design significantly influences the localized deposition of therapeutic agents within the vascular wall [191].

After release from the stent coating, the drug must be further transported within the vascular wall to reach target cells. This process is jointly regulated by diffusion, convection, and binding kinetics to tissue components, with their relative importance depending on drug properties and tissue characteristics. Diffusion is the fundamental mode of drug transport in the vascular wall, driven by concentration gradients. Using a cylindrical diffusion model, Zhao et al. further demonstrated that the effective diffusion coefficient of the drug in tissue determines its spatiotemporal profile in the vascular wall: a higher coefficient yields an earlier and higher peak tissue concentration but faster clearance, whereas a lower coefficient delays and lowers the peak while prolonging tissue retention [186]. Mongrain et al. further investigated the relative importance of diffusion coefficients across the polymer coating, vascular wall, and blood domains, finding that the diffusion coefficients in the coating and vessel wall are the key parameters governing drug accumulation: smaller diffusion coefficients lead to higher drug accumulation and prolonged retention in the vascular wall, and the relative magnitudes of the coating and wall diffusion coefficients co-regulate the kinetics of drug uptake and clearance [192]. Pontrelli et al. established two-layer and multi-layer porous media diffusion models and, by deriving analytical solutions to the transient diffusion equation, obtained drug concentration distributions in each layer and estimated drug penetration depth in the arterial wall, thereby providing theoretical tools for analyzing the physical limits of drug diffusion [193,194]. Blood flow has a dual effect on drug delivery. On the one hand, luminal blood flow washes away most of the drug released from the stent surface, resulting in only a small fraction ultimately entering the vascular wall [192]. On the other hand, flow disturbance induced by stent struts creates micro-recirculation zones (drug pools) downstream, and drug released from the luminal side of struts contributes up to 43% of tissue drug deposition, indicating that these regions play a significant role in drug entry into the vascular wall [195]. Therefore, the net effect of blood flow on drug delivery depends on the balance between washout and drug pooling, and is modulated by drug lipophilicity/hydrophilicity [196]. Once inside the vascular wall, further drug transport is dominated by interstitial fluid flow, driven by Darcy flow arising from the transmural pressure gradient. Studies have shown that convection contributes more significantly to the transport of hydrophilic drugs, while having relatively less influence on hydrophobic drugs [196]. Formaggia et al. modeled the arterial wall as a homogeneous porous medium, accounting for drug diffusion, convection, and reversible binding to tissue constituents, thereby coupling the transport processes within the tissue domain to the coating release kinetics [188]. Vairo et al. developed a multi-domain convection-diffusion model that comprehensively accounted for the regulatory role of tissue microstructure on drug transport. Their results demonstrated that stronger axial than radial diffusion promotes more uniform drug distribution in the tissue, while porosity and protein binding jointly regulate drug retention time [197]. O'Brien et al. further investigated the influence of pulsatile blood flow on drug distribution, revealing a complex interaction between pulsatility and stent malapposition: for mildly malapposed struts, reducing the pulsatile frequency increased drug uptake by approximately 10%, whereas for moderately malapposed struts, the same frequency change decreased drug uptake by 33% [198]. Bozsak et al. compared the transport behavior of paclitaxel and sirolimus in the arterial wall, finding that the former is dominated by convection, while the latter is primarily governed by binding processes [199].

 doi:10.20944/preprints202606.0497.v1

Binding kinetics simulations quantify the dynamic binding and dissociation processes between drugs and tissue constituents by establishing reversible reaction models. As shown in Figure 4C, after entering the vascular wall, drugs exist partially in the free form, while the remainder binds to tissue components (e.g., receptors) to form the bound state, constituting a dynamically reversible interconversion process termed the two-phase delivery mechanism. The dynamic equilibrium between these two states jointly determines drug distribution and retention within the tissue [14]. Borghi et al. pioneered the reversible chemical reaction model to describe the interaction between hydrophilic drugs and vascular wall binding sites. This model revealed a local "reservoir effect", i.e., the drug initially binds to these sites and subsequently undergoes slow dissociation, thereby prolonging its residence time within the tissue [200]. Formaggia et al. first incorporated reversible binding reactions into the arterial wall tissue module, laying the foundational framework for multi-domain coupled drug delivery models [188]. McGinty and Pontrelli further compared specific and non-specific binding models and concluded that a two-phase binding model more accurately captures the spatiotemporal distribution of drug binding to specific receptors, whereas a single-phase model is adequate for matching total tissue drug mass experiments [201]. Tzafriri et al. introduced the concept of "binding potential" to elucidate the threshold-dependent nature of arterial drug transport [202]. Bozsak et al. further demonstrated that sirolimus transport in the arterial wall is primarily governed by binding interactions, whereas paclitaxel transport is dominated by convective transport [199]. Saha et al. characterized the spatiotemporal dynamics of gradual binding site saturation in the vessel wall [203]. Mandal et al. identified a significant negative correlation between atherosclerotic plaque thickness and the concentration of bound drug [204]. Collectively, these binding kinetics models provide a robust theoretical foundation for understanding drug distribution and retention in arterial tissues, as well as actionable guidance for the rational design of targeted delivery strategies. Targeted delivery simulations are designed to model the active recognition process between drug carriers and specific receptors on vascular cell surfaces, enabling precise spatiotemporal drug delivery. In the field of magnetic targeting, Wang et al. developed a multi-physics coupled model to simulate the targeted delivery of drug-loaded magnetic nanoparticles to stent surfaces under an applied external magnetic field. They systematically analyzed the effects of magnetic field strength, nanoparticle size, and blood flow velocity on particle capture efficiency, providing quantitative guidance for the optimization of magnetic drug delivery systems [205]. Looking ahead, the integration of multiscale modeling approaches, from molecular recognition to macroscopic transport, holds great promise for developing comprehensive computational tools for the rational design of targeted stent coatings.

4.3.2. Modulation of Drug Delivery by Carrier and Stent Design

The efficiency of stent-based drug delivery to local tissues depends not only on the physicochemical properties of the drug itself, but is also profoundly governed by the carrier structure, material characteristics, and stent geometric design. Computational simulations enable the systematic evaluation of how various design parameters influence release kinetics, tissue transport, and binding processes, thereby providing a theoretical basis for stent optimization. The choice of carrier material and its structural design largely dictate the drug release kinetics, representing a primary consideration in the design of drug delivery systems. Material type exerts a fundamental impact on release behavior. Biodegradable and non-biodegradable coatings exhibit distinctly different release profiles. By establishing simulation models, Sarifuddin et al. systematically compared the impacts of biodegradable, biostable, and polymer-free coatings on drug release, and the results showed that biodegradable coatings exhibit the most rapid drug release, whereas biostable coatings achieve a quasi-steady state (i.e., a state in which drug concentration remains relatively constant over time regardless of the degree of strut embedment), thereby demonstrating more prolonged local delivery characteristics [206]. Furthermore, the structural design of coatings offers greater degrees of freedom for modulating drug release. Sarifuddin et al. developed a computational model for bilayer coatings to elucidate the synergistic mechanism between the base and top layers,

 doi:10.20944/preprints202606.0497.v1

demonstrating that optimizing the kinetic parameters of both layers can significantly enhance drug delivery efficiency [207]. Porous architectures introduce an additional dimension for regulating drug release. By modeling the coating as a porous reservoir, Pontrelli et al. numerically solved the local non-equilibrium diffusion problem within porous media; their findings revealed that the delay in drug release is governed by the interplay between the physicochemical properties of the drug and the coating microstructure, thereby providing a theoretical foundation for utilizing porous carriers in drug-eluting stents [208].

Stent geometric parameters directly influence the transport pathways and spatial distribution of drugs within the tissue, representing a critical factor governing the spatial uniformity of drug delivery. This section focuses on how these geometric parameters dictate the subsequent transport behavior of therapeutic agents in the tissue. Stent geometry and connector design are primary determinants of drug release. Chen et al. found through numerical simulations that longitudinal connector designs are more effective as drug-release carriers, while excessive connector density hinders drug release [209]. Additionally, Vijayaratnam et al. utilized CFD to show that streamlined stent strut designs can simultaneously reduce coating volume and increase the coating-tissue contact area, thereby improving hemodynamics and enhancing drug uptake [210]. Inter-strut distance exerts a profound influence on the spatial distribution of drugs within the vascular wall. Mandal et al. systematically investigated this effect through numerical simulations, revealing that at small inter-strut distances, overlapping concentration profiles merge into a single broad peak. Conversely, as the distance increases, distinct concentration peaks emerge above each individual strut, highlighting inter-strut distance as a key geometric parameter for regulating spatial uniformity [211]. Furthermore, another CFD study examining curved arteries confirmed that drug deposition increases with greater inter-strut spacing [212]. The degree of compression exerted by stent struts on the vascular wall dictates the initial pathways for drug entry into the tissue. O'Connell et al. investigated idealized stent configurations and concluded that strut designs imposing less tissue compression significantly improve the spatial uniformity of drug distribution within the vascular wall [213].

Computational design approaches enable the intuitive and accurate prediction of structural mechanical responses, local hemodynamic states, and spatial delivery behaviors of therapeutic agents under complex parameter configurations. Through systematic evaluation of synergistic multi-factor effects and multi-objective optimization, these simulations provide a scientific basis for vascular stent design and offer valuable guidance toward personalized stent applications for individual patients in clinical practice.

5. Potential Clinical Applications of Vascular Stents

The clinical value of vascular stents lies in reconstructing blood flow pathways via mechanical support, thereby treating vascular stenosis, occlusion or structural abnormalities caused by diverse etiologies. Figure 4 highlights representative studies on four typical clinical applications of vascular stents [214–217]. This section provides a comprehensive review of the potential clinical applications of vascular stents.

5.1. Atherosclerotic Vascular Disease

The application of vascular stents in atherosclerotic vascular disease has developed into a well-established therapeutic strategy, with its safety and efficacy validated in numerous clinical studies. With advances in materials science and interventional technology, the clinical indications of vascular stents continue to expand, providing diverse therapeutic options for the management of atherosclerotic diseases.

 doi:10.20944/preprints202606.0497.v1

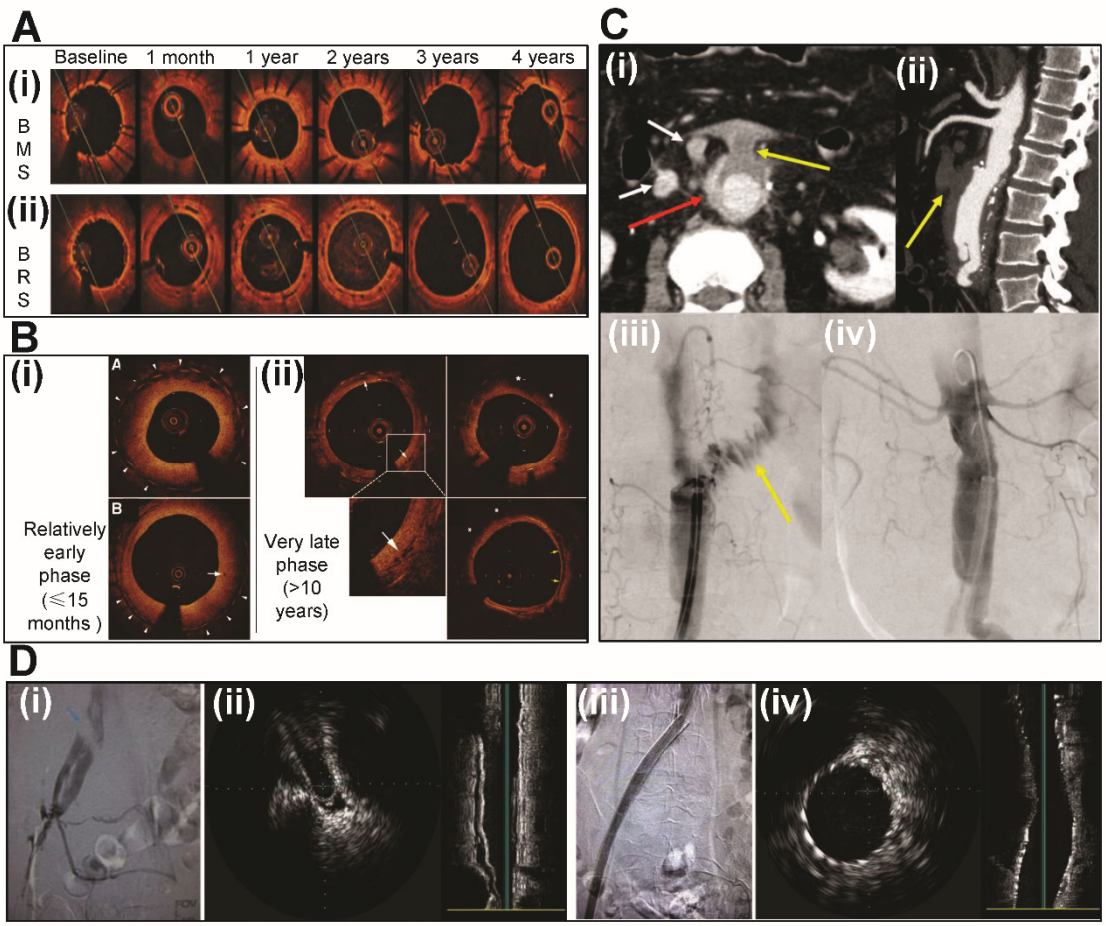

Figure 4. Potential clinical applications and imaging evaluation of vascular stents in different vascular beds. (A) Coronary artery atherosclerosis: Serial optical coherence tomography (OCT) over 4 years comparing (i) BMS and (ii) BRS. BMS maintain stable lumens; BRS enlarge (2–4 years) via remodeling and plaque regression [214]. (B) Peripheral artery atherosclerosis: OCT of BMS responses at (i) Relatively early (≤15 months) and (ii) very late (>10 years) phases. Relatively early phase shows peri-strut low-intensity areas (PLIA, arrowheads) and microvessels; very late phase shows neoatherosclerosis with lipid-rich intima (asterisks) and calcium (yellow arrows) [215]. (C) Aortic atherosclerosis: Computed tomography angiography (CTA) (i, ii) and digital subtraction angiography (DSA) (iii, iv). (i) Axial CTA shows infected anastomotic pseudoaneurysm (red arrow), partially thrombosed aorto-duodenal fistula (yellow arrow), and periaortic lymphadenopathy (white arrows). (ii) Sagittal CTA shows fistula extent (yellow arrow). (iii) Pre-interventional DSA confirms duodenal contrast extravasation (yellow arrow). (iv) Post-interventional DSA shows fistula sealed by endoprosthesis [216]. (D) Other vascular diseases (May-Thurner syndrome): Venography and intravascular ultrasound (IVUS). (i) Pre-interventional venography shows left common iliac vein compression by the right common iliac artery with collaterals. (ii) Pre-interventional IVUS confirms narrowed lumen. (iii) Post-interventional venography shows patent inferior vena cava flow. (iv) Post-interventional IVUS verifies optimal stent expansion, wall apposition, and venous caliber [217].

5.1.1. Coronary Artery Atherosclerosis

Coronary artery atherosclerosis represents the most classic and widely utilized clinical domain for vascular stents. DES have effectively addressed the high incidence of postoperative restenosis [218], thereby significantly improving the clinical outcomes of percutaneous coronary interventions (PCI) [219] and fundamentally revolutionizing the management of coronary atherosclerosis [220]. Notably, vascular stents play a pivotal role in the treatment of both stable coronary artery disease and acute coronary syndromes. In patients with stable coronary artery disease, stent implantation is primarily performed to relieve symptoms and improve quality of life. Small-vessel disease is a

 doi:10.20944/preprints202606.0497.v1

common anatomical subset in patients with coronary artery disease [221]. Compared with durable polymer DES widely used in this setting, biodegradable polymer DES have shown favorable efficacy in managing small-vessel lesions [222]. Furthermore, clinical research on the use of bioresorbable scaffolds in stable coronary artery disease is ongoing. Silent myocardial ischemia is an important manifestation of stable coronary artery disease [223]. Clinical trials of DES have enrolled patients with silent myocardial ischemia, showing that stent implantation is associated with exceptionally low rates of myocardial infarction and stent thrombosis, along with favorable angiographic and major adverse cardiac event outcomes [224]. Left main and multivessel disease are high-risk anatomical subsets of stable coronary artery disease [225]. Studies have demonstrated that DES implantation yields sustained improvements in quality of life in patients with triple-vessel and left main disease [226].

Acute coronary syndromes (ACS) represent high-acuity clinical scenarios for stent intervention, comprising ST-segment elevation myocardial infarction (STEMI), non-ST-segment elevation myocardial infarction (NSTEMI), and unstable angina (UA) [227]. In patients with STEMI, primary PCI serves as the cornerstone reperfusion strategy. Clinical studies have shown that BRS technology, through optimized design combined with intravascular imaging guidance, can achieve complete resorption without permanent metallic implants, effectively mitigating thrombotic risk while preserving physiological vasomotor function [214]. In patients with STEMI, BRS has demonstrated clinical outcomes comparable to those of patients treated with everolimus-eluting stents [228]. For patients with NSTEMI, implantation of new-generation DES significantly improves long-term prognosis. Evidence demonstrates that new-generation DES are associated with a significantly lower risk of major adverse cardiac events (MACE) compared with bare-metal stents [229], as well as a 29% reduction in the 5-year risk of heart failure hospitalization in NSTEMI patients [230]. Similarly, stent implantation constitutes a cornerstone therapy for patients with UA. A 10-year follow-up study revealed that new-generation DES significantly reduce the risks of target lesion revascularization, target vessel revascularization, and MACE, thereby conferring superior long-term clinical efficacy [231].

5.1.2. Peripheral Artery Atherosclerosis

Peripheral artery atherosclerosis represents a major application domain for vascular stents, with femoropopliteal, infrapopliteal, and iliac artery disease constituting typical anatomical subsets [232]. Critical limb ischemia, a severe manifestation of peripheral artery disease, represents a leading cause of amputation, wherein stent implantation is indicated to achieve limb salvage and optimize patient prognosis [233]. Infrapopliteal artery atherosclerosis remains a significant therapeutic challenge, which is particularly prevalent in patients with diabetes mellitus [234]. A meta-analysis demonstrated that bioresorbable scaffolds implanted in infrapopliteal arteries achieved a 1-year primary patency rate of approximately 90% and a freedom from target lesion revascularization (TLR) of 96%, indicating favorable short-term clinical outcomes [235]. Concurrently, femoropopliteal lesions are exposed to complex dynamic mechanical stresses, including bending, compression, and torsion, which contribute to a relatively high rate of stent fracture [236]. Within this segment, optical coherence tomography evaluation of bare-metal stents deployed in the superficial femoral artery has demonstrated that peri-strut low-intensity areas (PLIA) are universally present in the early phase, while in-stent neoatherosclerosis develops in the very late phase, reflecting the vascular healing characteristics of this peripheral arterial bed [215]. DES technology has significantly enhanced therapeutic efficacy for femoropopliteal disease, with data showing a 1-year clinical patency rate of 84% and a freedom from TLR of 89%, thereby confirming satisfactory postprocedural recovery [237]. For iliac artery atherosclerosis, endovascular stenting yields excellent outcomes and represents a highly mature clinical domain. The SENS-ILIAC randomized controlled trial demonstrated a 1-year clinical patency rate of up to 99% for iliac artery stenting, confirming its role as a highly effective intervention for atherosclerotic occlusive disease [238]. Furthermore, even in severely calcified

 doi:10.20944/preprints202606.0497.v1

lesions, stent implantation maintains a 1-year patency rate of 93% and a freedom from TLR of 98%, demonstrating favorable safety profiles and durable clinical efficacy [239].

5.1.3. Aortic Atherosclerosis

Covered stent grafts represent a critical therapeutic modality for conditions associated with aortic atherosclerosis. Numerous studies have confirmed favorable clinical outcomes after stent deployment in patients treated with these devices. The pathogenesis of abdominal aortic aneurysms and certain types of aortic dissection is closely associated with aortic atherosclerosis [240,241]. Studies have shown that patients with ruptured abdominal aortic aneurysms treated with covered stent grafts exhibit significantly lower 30-day mortality compared with those undergoing open surgery [242]. For thoracoabdominal aortic aneurysms, endovascular repair with covered stent grafts achieved a 12-month branch vessel patency rate of 96.7% and an overall survival rate of 98.6%, demonstrating favorable safety and efficacy profiles [243]. For complex dissections involving the aortic arch and descending thoracic aorta, the frozen elephant trunk technique combined with stent implantation offers a novel surgical alternative [244].

Notably, computed tomography angiography (CTA) remains indispensable during postoperative follow-up following endovascular interventions. Evidence demonstrates that for patients following stent graft repair, particularly in abdominal aortic disease, CTA is essential to systematically assess stent morphology and precisely identify critical complications such as endoleak, stent migration, graft infection, and secondary aortoenteric fistula, thereby providing a structured evaluative framework for long-term surveillance [216].

5.2. Other Vascular Diseases

Beyond atherosclerotic vascular disease, vascular stents have also demonstrated favorable therapeutic efficacy across a diverse spectrum of other disorders, including inflammatory vascular diseases and vascular compression syndromes. This section provides a comprehensive review of these clinical applications. Inflammatory vascular diseases, such as Takayasu arteritis [245] and cerebral vasculitis [246], can lead to vascular stenosis and occlusion. When medical therapy is ineffective, stent implantation can serve as a salvage treatment. A published case report has demonstrated that a patient with Takayasu arteritis remained free of restenosis or reocclusion at 2-year follow-up after stent implantation, indicating that vascular stent therapy can yield a favorable prognosis during the stable phase of inflammation [247]. For cerebral vasculitis refractory to medical treatment, stent implantation provides a salvage treatment option, and its combination with intensive medical therapy has demonstrated favorable clinical outcomes [248]. In patients with Behçet disease on immunosuppressive therapy, stent placement for occluded common femoral and iliac veins has been reported to achieve successful recanalization [249]. Vascular compression syndromes represent a group of disorders caused by the extrinsic compression of blood vessels by surrounding anatomical structures, including May-Thurner syndrome and nutcracker syndrome [250]. May-Thurner syndrome is effectively managed with iliac vein stent implantation. Compared with balloon angioplasty alone, stent placement effectively resists the persistent mechanical compression from the overlying right common iliac artery. Furthermore, intraoperative guidance using intravascular ultrasound (IVUS) allows precise assessment of the degree of compression and optimizes stent sizing and positioning, thereby improving long-term primary patency rates [217]. Published studies report a 1-year primary patency rate of over 84% after stent implantation, effectively relieving lower extremity swelling and pain [251]. Similarly, nutcracker syndrome is also amenable to endovascular stent placement. In a recent series of patients treated with either surgical transposition or stenting, the overall 1-year primary patency rate was 87%, with symptom relief rates exceeding 80% for both flank pain and hematuria [252]. Furthermore, vascular stents play a critical therapeutic role in the management of vascular injuries, congenital vascular malformations, and post-transplantation vascular complications. For vascular injuries, stents are particularly useful for managing iatrogenic injuries, including iliac artery occlusion after laparoscopy [253], arteriovenous fistulas following

 doi:10.20944/preprints202606.0497.v1

lumbar surgery [254], and high-output heart failure caused by arteriovenous fistulas after lumbar disc surgery [255]. For congenital vascular malformations, stenting is a key interventional modality, especially in pediatric patients, as it can delay or obviate the need for complex open surgery. Successful stent implantation has been reported in multiple conditions, including coarctation of the aorta [256], branch pulmonary artery stenosis after complex congenital heart disease repair [257]. For post-transplantation vascular complications, stents offer a minimally invasive salvage therapy. Complications including transplant renal artery stenosis [258], hepatic artery stenosis after liver transplantation [259], and iliac artery lesions after pancreas transplantation can all be successfully managed with stent implantation [260].

The clinical applications reviewed span a broad spectrum of vascular diseases. Across all these clinical scenarios, vascular stents have consistently demonstrated therapeutic value beyond mechanical support, encompassing drug delivery, local pathology management, and minimally invasive vascular reconstruction. Nevertheless, challenges remain in achieving personalized design, reliable long-term outcome prediction, and precise spatiotemporal control over drug delivery. The following section explores how artificial intelligence can address these challenges and usher in a new era of intelligent, personalized vascular interventions.

6. Future Perspectives in Vascular Stent Development

The core missions of vascular stents encompass restoring vascular integrity, optimizing hemodynamics, and providing therapeutic functionality through controlled drug delivery. Together, these functions determine their clinical efficacy of stent-based interventions. With the rapid advancement of artificial intelligence, its profound integration across materials development, carrier design, and optimization via simulation is paving new pathways toward the ultimate realization of precision clinical decisions.

In the realm of stent materials development, as discussed in preceding sections, biodegradable metallic stents face the challenge of balancing degradation kinetics, while polymeric stents are constrained by inherent mechanical limitations. Data-driven strategies are therefore emerging as powerful tools to address these long-standing challenges. . By constructing quantitative relationships among material composition, processing parameters, and performance, machine learning enables rapid screening of optimal formulations from large compositional spaces thereby shifting the paradigm of alloy stent design from empirical exploration to predictive precision [261,262],. This data-driven methodology has been successfully extended to titanium alloys and other metallic material systems, significantly expanding the design space for intelligent vascular stent materials [263,264] Recently, the integration of deep learning with high-resolution imaging enables quantitative characterization of the in vivo stent degradation behavior, providing a novel evaluative tool for the precise modulation of degradation [265],. Lattice superstructures, a novel architectural configuration for metallic stents, have been optimized through machine learning-assisted design to achieve synergistic regulation of mechanical performance and superelasticity, thereby introducing a new paradigm of integrated structural-functional design for next-generation high-performance vascular stents [266]. In the polymeric domain, the application of machine learning to the optimization of polylactic acid properties has attracted increasing attention; by enhancing mechanical performance and refining processing parameters, novel strategies for the design of bioresorbable polymeric scaffolds are emerging [267]. Furthermore, the convergence of artificial intelligence with additive manufacturing is empowering the entire chain of stent fabrication, spanning compositional design, structural optimization, and process control [268]. It can be anticipated that, as data-driven methodologies become deeply integrated with materials science, artificial intelligence will accelerate the resolution of critical bottlenecks, including insufficient control over alloy stent degradation kinetics and inadequate mechanical support of polymeric stents, ultimately transforming on-demand design into a tangible reality. Achieving this goal, however, will depend not only on the powerful predictive capacity of machine learning but also on the development of interpretable models capable of elucidating the intrinsic relationships between material parameters and performance outcomes

 doi:10.20944/preprints202606.0497.v1

[267]. Such interpretability will facilitate the inverse design of optimal material formulations and architectures tailored to specific clinical requirements, including predetermined support duration, degradation profiles, and mechanical demands, thereby providing an essential reference framework for the development of next-generation biodegradable, high-performance vascular stents.

In the realm of carrier functional design, hydrogels, fibers, nanoparticles, microspheres, and other carriers endow vascular stents with multiple biological functions, including anti-proliferative, anticoagulant, and pro-endothelialization activities. Recent research has demonstrated a distinct trend from single-agent release toward multi-drug synergistic delivery, and from passive release toward targeted delivery, while temporally regulated strategies are being actively explored in cutting-edge domains such as gas-based therapeutics. The integration of artificial intelligence is accelerating this paradigm shift. Specifically, regarding intelligent carrier design and screening, machine learning can assist in designing stimuli-responsive materials and optimizing the mechanical properties, degradation kinetics, and release profiles of hydrogels, thereby opening new avenues for personalized, on-demand release strategies in the design of stent coating carriers [86].

In the realm of biomimetic carriers and smart structures, the convergence of AI with nanoengineering, 4D printing, and other advanced technologies is creating carrier systems with dynamic and stimuli-responsive functionalities. Biomimetic carriers, exemplified by exosome-mimetic nanovesicles, can achieve more precise targeted delivery and immunomodulation, while the integration of artificial intelligence-assisted design offers new opportunities for their personalized application and optimization [269]. In terms of carrier performance evaluation, machine learning is substantially enhancing computational efficiency. Artificial intelligence technologies can be deployed across the entire lifecycle of vascular stent carrier, thereby demonstrating the potential for end-to-end empowerment from carrier design to clinical application [270]. As artificial intelligence becomes deeply integrated with carrier engineering, vascular stent carriers are rapidly evolving from passive release platforms toward intelligent responsive systems. This transformation relies not only on the precise prediction of carrier material properties through machine learning but, more critically, on its capacity to uncover the complex relationships among carrier architecture, release behavior, and biological responses. It is anticipated that in the near future, intelligent carrier systems with programmed release kinetics can be inversely designed according to the temporal demands of vascular injury repair, thereby providing pivotal support for the development of next-generation personalized, temporally sequenced vascular therapeutics.

In the realm of personalized stent design, the convergence of artificial intelligence with patient-specific data is opening new frontiers. Deep learning models trained on medical imaging data can rapidly reconstruct patient-specific vascular anatomies and automatically identify lesion characteristics, such as the degree of calcification and plaque composition, thereby providing a precise basis for stent selection and implantation strategies [271]. Furthermore, frameworks integrating finite element simulation with machine learning can predict the deployment configuration and mechanical compatibility of various stent designs in patient-specific vascular anatomies [272], enabling interventionalists to preoperatively simulate procedural outcomes and select optimal stent configurations through virtual surgical planning platforms tailored to patient-specific anatomy. Moreover, the fusion of digital twin technology with artificial intelligence holds promise for enabling real-time intraoperative feedback. For the interventional treatment of coronary bifurcation lesions, a framework combining hemodynamic simulation with machine learning can provide real-time assessment of functional flow indices of the side branch following stent implantation, thereby reducing periprocedural uncertainty for each patient [273]. Underpinning these specific technologies is the integrated application of surrogate models, shape optimization, and patient-specific design methodologies, which together constitute a methodological framework for the rapid development of next-generation personalized stents [274]. Through the deep mining of patient-specific data and real-time functional assessment, artificial intelligence is propelling vascular stent interventions from population-based protocols toward individualized decision-making, better

 doi:10.20944/preprints202606.0497.v1

addressing the unique clinical needs of each patient and providing essential references for the personalized design of vascular stents and intraoperative clinical decision-making.

In the realm of prognostic prediction and risk stratification, artificial intelligence is transforming clinical assessment from post-hoc evaluation to proactive early warning. Machine learning models based on multimodal data, including medical imaging, biochemical markers, and clinical characteristics, can predict the risk of post-stenting complications such as restenosis and thrombosis, providing decision support for personalized anticoagulation and follow-up regimens [275,276]. Furthermore, previous studies have demonstrated that machine learning models based on imaging-derived digital twins can effectively predict the risk of endoleaks after vascular stent implantation [277]. At present, the integrated application of AI across key stages including design optimization of drug-coated cardiovascular devices, real-time imaging interpretation guidance, and postoperative complication prediction is demonstrating significant potential for end-to-end empowerment from bench to bedside [270]. Collectively, these technologies are driving the integration of risk warning throughout the entire patient treatment cycle, spanning preoperative planning to postoperative follow-up, thereby delivering comprehensive clinical care support.

Artificial intelligence is comprehensively reshaping the research, development, and application paradigms of vascular stents across materials science, carrier design, simulation optimization, clinical decision-making, and prognostic management. The on-demand design of materials, intelligent responsiveness of carriers, intelligent prediction of simulations, individualized decision-making in clinical practice, and comprehensive early warning in prognosis are interwoven and evolving synergistically, collectively propelling vascular stents into a new era of intelligence and precision. With the deep integration of artificial intelligence with materials science, carrier technology, biomechanics, and clinical medicine, vascular stents will gradually achieve integrated intelligent design that unifies structure, function, and therapeutic efficacy. In the future, research efforts are expected to rapidly iterate optimal vascular stent design solutions in virtual environments based on individual patient characteristics, and further advance the realization of real-time intraoperative adjustment of interventional strategies, thereby bringing safer, more precise, and more personalized therapeutic prospects to patients with cardiovascular diseases.

Conflicts of Interest: The authors declare no conflict of interest.

Acknowledgments: This work was supported by the Fundamental Research Funds for the Central Universities.

References

1. Amjad, H.; Ullah, A.; Shakoor, M.; Tanveer, F.; Qureshi, M.; Jahan, F.; Manzoor, H.; Mahmoud, M.H.; Masharifa Ahamed, F.; Halder, A.; et al. Comparative Efficacy and Long-Term Outcomes of Drug-Eluting Stents vs. Bare-Metal Stents in Coronary Artery Disease: A Systematic Review. *Cureus* **2025**, *17*, e86617, doi:10.7759/cureus.86617.
2. Im, S.; Im, D.; Park, S.; Jung, Y.; Kim, D.; Kim, S. Current Status and Future Direction of Metallic and Polymeric Materials for Advanced Vascular Stents. *Prog. Mater. Sci.* **2022**, *126*, doi:10.1016/j.pmatsci.2022.100922.
3. Flowers, A.; Evenhuis, B.; Gabanic, B.; Weiss, A.; Eisenberg, S.; Siddiqui, R.; Rizwan, A.; Riaz, I.; Virk, H.; Alam, M.; et al. Stent Thrombosis: A Contemporary Guide to Definitions, Risk Factors, and Management. *Front. Cardiovasc. Med.* **2025**, *12*, doi:10.3389/fcvm.2025.1622235.
4. Liu, B.; Li, M.; Liu, J.; Xie, L.; Li, J.; Liu, Y.; Niu, C.; Xiao, D.; Li, J.; Zhang, L. Risk Factors and Incidence for In-Stent Restenosis with Drug-Eluting Stent: A Systematic Review and Meta-Analysis. *Rev. Cardiovasc. Med.* **2024**, *25*, doi:10.31083/j.rcm2512458.
5. Farhan, M.; Hasan, G.; Sobhi, A.; Yasser, K.; Humam, M.; Ali, M.; Younes, S.; Nazir, M.H.; Mateen, M.A.; Misra, G.; et al. Bioresorbable Scaffolds Advances, Challenges, and Future Directions. *Ann. Med. Surg. 2012* **2025**, *87*, 4173–4183, doi:10.1097/MS9.0000000000003424.

 doi:10.20944/preprints202606.0497.v1

6. Galassi, L.; Verri, M.G.; Bartolozzi, H.; Verrengia, A.; Facchinetti, F.; Ravini, M.L. Bioresorbable Scaffolds in Lower Limb Arterial Disease: A Narrative Review of Advancements and Future Directions. *Vessel Plus* **2026**, *10*, 6, doi:10.20517/2574-1209.2025.85.
7. Cho, L.D.; Parikh, S.A. Next-Generation Drug Delivery Systems and Drugs for Vascular Intervention. *Interv. Cardiol. Clin.* **2026**, *15*, 307–318, doi:10.1016/j.iccl.2025.12.010.
8. Jadhav, S.A.; Raval, A.J.; Patravale, V.B. Drug Delivery, Development, and Technological Aspects for Peripheral Drug Eluting Stents. *Adv. Drug Deliv. Rev.* **2025**, *226*, 115678, doi:10.1016/j.addr.2025.115678.
9. Tan, J.; Wang, H.; Liu, S.; Li, L.; Liu, H.; Liu, T.; Chen, J. Multifunctional Nanocoatings with Synergistic Controlled Release of Zinc Ions and Cytokines for Precise Modulation of Vascular Intimal Reconstruction. *Nanomedicine Nanotechnol. Biol. Med.* **2024**, *57*, 102739, doi:10.1016/j.nano.2024.102739.
10. Song, D.H.; Baik, S.; Kim, J.Y.; Park, J.M.; Ryu, B.; Seo, I.H.; Lee, S.S.; Kim, H.B.; Hong, Y.J.; Koh, W.-G.; et al. Multilayer Surface Coating for Enhanced Anti-Inflammation, Anti-Restenosis, and Re-Endothelialization in Advanced Biodegradable Vascular Stents. *Mater. Today Bio* **2025**, *35*, 102570, doi:10.1016/j.mtbio.2025.102570.
11. Wang, C.; Lv, J.; Yang, M.; Fu, Y.; Wang, W.; Li, X.; Yang, Z.; Lu, J. Recent Advances in Surface Functionalization of Cardiovascular Stents. *Bioact. Mater.* **2025**, *44*, 389–410, doi:10.1016/j.bioactmat.2024.10.025.
12. Corti, A.; Dal Ferro, L.; Akyildiz, A.C.; Migliavacca, F.; McGinty, S.; Chiastra, C. Plaque Heterogeneity Influences In-Stent Restenosis Following Drug-Eluting Stent Implantation: Insights from Patient-Specific Multiscale Modelling. *J. Biomech.* **2025**, *179*, 112485, doi:10.1016/j.jbiomech.2024.112485.
13. Li, S.; Wei, Y.; Li, H. A Numerical Study on the Drug Release Process of Biodegradable Polymer Drug-Loaded Vascular Stents. *Polymers* **2025**, *17*, doi:10.3390/polym17030420.
14. Saha, R.; Mandal, A.P.; Mandal, P.K. Physiological Consequences of Half-Embedded Drug-Eluting Stent on Coronary Drug-Transport: A Two-Species Drug Delivery Simulation. *Med. Eng. Phys.* **2025**, *139*, 104334, doi:10.1016/j.medengphy.2025.104334.
15. Saha, R.; Choudhury, S. Computational Modeling of Luminal Flow-Driven Mass Transport in Coronary Arteries for Optimizing Drug-Eluting Stent Efficacy. *Indian J. Physiol. Allied Sci.* **2026**, *78*, 18–25, doi:10.55184/ijpas.v78i01.546.
16. Qiu, J.; Tang, L.; Fu, W.; Qin, L.; Zhang, D.; Wang, S.; Song, J. Enhancing Radial Strength and Expansion Uniformity of Iron-Based Vascular Scaffolds: A Numerical and Experimental Investigation on Topological Optimization. *Front. Bioeng. Biotechnol.* **2025**, *13*, 1736027, doi:10.3389/fbioe.2025.1736027.
17. Zhao, G.; Zhang, Z.; Chen, E.; Ding, F.; Yuan, R.; Song, C.; Yan, W.; Wu, K.; Wu, J. Mechanical Characteristics of Braided Composite Stents for Carotid Artery Stenosis Using Finite Element Method. *Comput. Methods Biomech. Biomed. Engin.* **2025**, 1–9, doi:10.1080/10255842.2025.2471501.
18. McCarthy, R.P.; Mason, P.J.; Marks, D.S.; LaDisa, J.F.J. Influence of Boundary Conditions and Blood Rheology on Indices of Wall Shear Stress from IVUS-Based Patient-Specific Stented Coronary Artery Simulations. *Sci. Rep.* **2025**, *15*, 15868, doi:10.1038/s41598-025-99066-w.
19. Shah, I.; Molony, D.; Lefieux, A.; Crawford, K.; Piccinelli, M.; Sun, H.; Giddens, D.; Samady, H.; Veneziani, A. Impact of the Stent Footprint on Endothelial Wall Shear Stress in Patient-Specific Coronary Arteries: A Computational Analysis from the SHEAR-STENT Trial. *Comput. Methods Programs Biomed.* **2025**, *266*, 108762, doi:10.1016/j.cmpb.2025.108762.
20. Ranno, A.; Manjunatha, K.; Koritzius, T.; Steinbrecher, I.; Hosters, N.; Nachtsheim, M.; Nilcham, P.; Schaaps, N.; Turoni-Glitz, A.; Datz, J.; et al. A Computational Model of Coronary Arteries with In-Stent Restenosis Coupling Hemodynamics and Pharmacokinetics with Growth Mechanics. *Sci. Rep.* **2025**, *15*, 39229, doi:10.1038/s41598-025-22291-w.
21. Saha, R.; Choudhury, S. Modeling Receptor-Mediated Drug Delivery Influenced by Non-Specific Binding in Stenosed Arterial Walls with Atherosclerotic Plaques. *Indian J. Physiol. Allied Sci.* **2025**, *77*, 48–54, doi:10.55184/ijpas.v77i04.533.
22. Damrongwatanasuk, R.; Pollanen, S.; Bae, J.Y.; Wen, J.; Nanna, M.G.; Damluji, A.A.; Mamas, M.A.; Hanna, E.B.; Hu, J.-R. Coronary Bifurcation PCI-Part II: Advanced Considerations. *J. Cardiovasc. Dev. Dis.* **2025**, *12*, doi:10.3390/jcdd12110439.

 doi:10.20944/preprints202606.0497.v1

23. Mutlu, O.; Salman, H.E.; Al-Thani, H.; El-Menyar, A.; Qidwai, U.A.; Yalcin, H.C. How Does Hemodynamics Affect Rupture Tissue Mechanics in Abdominal Aortic Aneurysm: Focus on Wall Shear Stress Derived Parameters, Time-Averaged Wall Shear Stress, Oscillatory Shear Index, Endothelial Cell Activation Potential, and Relative Residence Time. *Comput. Biol. Med.* **2023**, *154*, 106609, doi:10.1016/j.compbiomed.2023.106609.
24. Song, K.; Bi, Y.; Zhao, H.; Wu, T.; Xu, F.; Zhao, G. Structural Optimization and Finite Element Analysis of Poly-l-Lactide Acid Coronary Stent with Improved Radial Strength and Acute Recoil Rate. *J. Biomed. Mater. Res. B Appl. Biomater.* **2020**, *108*, 2754–2764, doi:10.1002/jbm.b.34605.
25. Miao, J.; Huang, S.; Chen, Z.; Wang, Q.; Li, H. Structural Design and Mechanical Properties of Metal Vascular Stents Fabricated via Laser Powder Bed Fusion. *ACS Omega* **2025**, *10*, 51779–51790, doi:10.1021/acsomega.5c07808.
26. Sun, L.; Zeng, Y.; Shen, Z.; Yue, C.; Yang, Y.; Gao, J.; Zhang, J.; Yuan, Q.; Cha, L. Biodegradable Metal-Based Stents: Advances, Challenges, and Prospects. *J. Funct. Biomater.* **2025**, *16*, doi:10.3390/jfb16090315.
27. Saidi-Seresht, S.; von Koch, S.; Erlinge, D.; James, S.; Koul, S.; Grimfjärd, P. Long-Term Outcome of Percutaneous Coronary Intervention Using Absorb Bioresorbable Scaffold: A SCAAR Study. *J. Soc. Cardiovasc. Angiogr. Interv.* **2025**, *4*, 103724, doi:10.1016/j.jscai.2025.103724.
28. Jorge, C.; Dubois, C. Clinical Utility of Platinum Chromium Bare-Metal Stents in Coronary Heart Disease. *Med. Devices Auckl. NZ* **2015**, *8*, 359–367, doi:10.2147/MDER.S69415.
29. Bourazana, A.; Briasoulis, A.; Kourek, C.; Kuno, T.; Leventis, I.; Pantsios, C.; Androutsopoulou, V.; Spiliopoulos, K.; Giamouzis, G.; Skoularigis, J.; et al. Bioresorbable Scaffolds for Coronary Revascularization: From Concept to Clinical Maturity. *J. Cardiovasc. Dev. Dis.* **2025**, *13*, doi:10.3390/jcdd13010002.
30. Niu, J.; Huang, H.; Pei, J.; Jin, Z.; Guan, S.; Yuan, G. Research and Development Strategy for Biodegradable Magnesium-Based Vascular Stents: A Review. *Biomater. Transl.* **2021**, *2*, 236–247, doi:10.12336/biomatertransl.2021.03.06.
31. Duan, X.; Yang, Y.; Zhang, T.; Zhu, B.; Wei, G.; Li, H. Research Progress of Metal Biomaterials with Potential Applications as Cardiovascular Stents and Their Surface Treatment Methods to Improve Biocompatibility. *Heliyon* **2024**, *10*, e25515, doi:10.1016/j.heliyon.2024.e25515.
32. Huang, Z.; Skarbek, C.; Li, Y.; Touma, J.; Desgranges, P.; Gallet, R.; Sénémaud, J. Evolution of Coronary Stents: From Birth to Future Trends. *J. Clin. Med.* **2025**, *15*, doi:10.3390/jcm15010047.
33. Li, J.; Hu, X.; Chen, Y.; Fan, D.; Tan, C.; Yang, S.; Wu, H.; Wang, Y.; An, Q.; Xiao, Z.; et al. Review of Recent Progress in Vascular Stents: From Conventional to Functional Vascular Stents. *Chin. Chem. Lett.* **2025**, *36*, 110492, doi:10.1016/j.cclet.2024.110492.
34. Pan Chen; LI Luhan; Fan Zhifang; CAO Jingjing; LI Hezong Advanced Progress in Surface Function Treatment of Metallic Vascular Stents. *Surf. Technol.* **2025**, *54*, 185–198, doi:10.16490/j.cnki.issn.1001-3660.2025.21.013.
35. Chichareon, P.; Katagiri, Y.; Asano, T.; Takahashi, K.; Kogame, N.; Modolo, R.; Tenekecioglu, E.; Chang, C.-C.; Tomaniak, M.; Kukreja, N.; et al. Mechanical Properties and Performances of Contemporary Drug-Eluting Stent: Focus on the Metallic Backbone. *Expert Rev. Med. Devices* **2019**, *16*, 211–228, doi:10.1080/17434440.2019.1573142.
36. Rodriguez-Granillo, A.M.; Mieres, J.; Fernandez-Pereira, C.; Sadouet, C.C.; Milei, J.; Swieszkowski, S.P.; Stutzbach, P.; Santaera, O.; Wainer, P.; Rokos, J.; et al. Randomized Clinical Trial Comparing Bare-Metal Stents Plus Colchicine Versus Drug-Eluting Stents for Preventing Adverse Cardiac Outcomes: Three-Year Follow-Up Results of the ORal Colchicine in Argentina (ORCA) Trial. *J. Clin. Med.* **2025**, *14*, doi:10.3390/jcm14092871.
37. O'Brien, B.; Carroll, W. The Evolution of Cardiovascular Stent Materials and Surfaces in Response to Clinical Drivers: A Review. *Acta Biomater.* **2009**, *5*, 945–958, doi:10.1016/j.actbio.2008.11.012.
38. Wilson, T.M.; Sarris-Michopoulos, P.M.; Siddiqui, R.; Ahmed, A.; Riaz, I.; Licitra, G.; Ossi, J.; Khawaja, M.; Fanaroff, A.C.; Maehara, A.; et al. Precision Management of Coronary In-Stent Restenosis. *Trends Cardiovasc. Med.* **2026**, *36*, 44–55, doi:10.1016/j.tcm.2025.07.009.

 doi:10.20944/preprints202606.0497.v1

39. Munteanu, A.E.; Badea, A.A.; Popescu, A.M.; Pleșa, F.C.; Stanciu, S.M. In-Stent Restenosis Pathophysiology and Risk Factors: A Comprehensive Review. *Med. Kaunas Lith.* **2026**, *62*, doi:10.3390/medicina62020345.
40. Farhan, S.; Hemetsberger, R.; Matiasek, J.; Strehblow, C.; Pavo, N.; Khorsand, A.; Petneházy, O.; Petrási, Z.; Kaider, A.; Glogar, D.; et al. Implantation of Paclitaxel-Eluting Stent Impairs the Vascular Compliance of Arteries in Porcine Coronary Stenting Model. *Atherosclerosis* **2009**, *202*, 144–151, doi:10.1016/j.atherosclerosis.2008.04.039.
41. Torii, S.; Jinnouchi, H.; Sakamoto, A.; Kutyna, M.; Cornelissen, A.; Kuntz, S.; Guo, L.; Mori, H.; Harari, E.; Paek, K.H.; et al. Drug-Eluting Coronary Stents: Insights from Preclinical and Pathology Studies. *Nat. Rev. Cardiol.* **2020**, *17*, 37–51, doi:10.1038/s41569-019-0234-x.
42. Sica, S.; Pratesi, G.; Rossi, G.; Ferraresi, M.; Lovato, L.; Volpe, P.; Fadda, G.F.; Ferri, M.; Rizza, A.; D'Oria, M.; et al. Proximal Sealing in the Aortic Arch for Inner Curve Disease Using the Custom Relay Scalloped and Fenestrated Stent Graft. *J. Vasc. Surg.* **2024**, *80*, 1317-1325.e2, doi:10.1016/j.jvs.2024.07.086.
43. Moravej, M.; Mantovani, D. Biodegradable Metals for Cardiovascular Stent Application: Interests and New Opportunities. *Int. J. Mol. Sci.* **2011**, *12*, 4250–4270, doi:10.3390/ijms12074250.
44. Zhang, J.; Chen, Z.; Rao, L.; He, Y. Coronary Bioresorbable Metallic Stents: Advancements and Future Perspectives. *J. Cardiol.* **2025**, *85*, 69–78, doi:10.1016/j.jjcc.2024.08.003.
45. Marsden Back, L.; Gentry-Maharaj, A.; Ladwiniec, A. The Safety and Efficacy Profile of Magnesium-Based Bioresorbable Coronary Stents as Compared to Poly-L-Lactic Acid-Based Bioresorbable and Contemporary Drug-Eluting Coronary Stents-A Systematic Review. *Cardiol. Res. Pract.* **2025**, *2025*, 7481956, doi:10.1155/crp/7481956.
46. Ni, J.; Wang, W.; Xu, H.; Jiang, M.; Liu, X.; Lou, Y.; Yan, J.; Chen, Y.; Zhang, X. A Biodegradable High-Purity Magnesium Closing Clip for General Surgery. *Acta Biomater.* **2026**, *212*, 829–843, doi:10.1016/j.actbio.2025.11.040.
47. Forkmann, C.; Pritsch, M.; Baumann-Zumstein, P.; Lootz, D.; Joner, M. In Vivo Chronic Scaffolding Force of a Resorbable Magnesium Scaffold. *J. Biomech.* **2024**, *164*, 111988, doi:10.1016/j.jbiomech.2024.111988.
48. Haude, M.; Toelg, R.; Lemos, P.A.; Christiansen, E.H.; Abizaid, A.; von Birgelen, C.; Neumann, F.-J.; Wijns, W.; Ince, H.; Kaiser, C.; et al. Sustained Safety and Performance of a Second-Generation Sirolimus-Eluting Absorbable Metal Scaffold: Long-Term Data of the BIOSOLVE-II First-in-Man Trial at 5 Years. *Cardiovasc. Revascularization Med. Mol. Interv.* **2022**, *38*, 106–110, doi:10.1016/j.carrev.2021.07.017.
49. Haude, M.; Wlodarczak, A.; van der Schaaf, R.J.; Torzewski, J.; Ferdinande, B.; Escaned, J.; Iglesias, J.F.; Bennett, J.; Toth, G.G.; Joner, M.; et al. A New Resorbable Magnesium Scaffold for de Novo Coronary Lesions (DREAMS 3): One-Year Results of the BIOMAG-I First-in-Human Study. *EuroIntervention J. Eur. Collab. Work. Group Interv. Cardiol. Eur. Soc. Cardiol.* **2023**, *19*, e414–e422, doi:10.4244/EIJ-D-23-00326.
50. Verheye, S.; Wlodarczak, A.; Montorsi, P.; Torzewski, J.; Bennett, J.; Haude, M.; Starmer, G.; Buck, T.; Wiemer, M.; Nuruddin, A.A.B.; et al. BIOSOLVE-IV-Registry: Safety and Performance of the Magmaris Scaffold: 12-Month Outcomes of the First Cohort of 1,075 Patients. *Catheter. Cardiovasc. Interv. Off. J. Soc. Card. Angiogr. Interv.* **2021**, *98*, E1–E8, doi:10.1002/ccd.29260.
51. Hassna, E.; Huang, Y.; Yan, T. Biodegradable Metals for Cardiovascular and Orthopaedic Implants: A Comparative Review of Magnesium, Iron and Zinc. *Met. Adv.* **2026**, *39*, 68–82, doi:10.1016/j.metadv.2025.12.001.
52. Chen, S.; Du, T.; Zhang, H.; Qi, J.; Zhang, Y.; Mu, Y.; Qiao, A. Methods for Improving the Properties of Zinc for the Application of Biodegradable Vascular Stents. *Biomater. Adv.* **2024**, *156*, 213693, doi:10.1016/j.bioadv.2023.213693.
53. Qian, Y.; Chen, Y.; Jiang, J.; Pei, J.; Li, J.; Niu, J.; Zhu, J.; Yuan, G. Biosafety and Efficacy Evaluation of a Biodegradable Zn-Cu-Mn Stent: A Long-Term Study in Porcine Coronary Artery. *Bioact. Mater.* **2025**, *45*, 231–245, doi:10.1016/j.bioactmat.2024.11.022.
54. Ma, J.; Zhao, N.; Zhu, D. Endothelial Cellular Responses to Biodegradable Metal Zinc. *ACS Biomater. Sci. Eng.* **2015**, *1*, 1174–1182, doi:10.1021/acsbiomaterials.5b00319.
55. Fu, J.; Su, Y.; Qin, Y.-X.; Zheng, Y.; Wang, Y.; Zhu, D. Evolution of Metallic Cardiovascular Stent Materials: A Comparative Study among Stainless Steel, Magnesium and Zinc. *Biomaterials* **2020**, *230*, 119641, doi:10.1016/j.biomaterials.2019.119641.

 doi:10.20944/preprints202606.0497.v1

56. Oliver, A.A.; Sikora-Jasinska, M.; Demir, A.G.; Guillory, R.J. 2nd Recent Advances and Directions in the Development of Bioresorbable Metallic Cardiovascular Stents: Insights from Recent Human and in Vivo Studies. *Acta Biomater.* **2021**, *127*, 1–23, doi:10.1016/j.actbio.2021.03.058.
57. Bai, C.; Feng, X.; Lan, L.; Zhou, C.; Zhang, H. Recent Advances and Perspectives in Bioresorbable Metal Coronary Drug-Eluting Stents. *Biomed. Mater.* **2025**, *20*, 032001, doi:10.1088/1748-605X/adc058.
58. Gunatillake, P.; Mayadunne, R.; Adhikari, R. Recent Developments in Biodegradable Synthetic Polymers. *Biotechnol. Annu. Rev.* **2006**, *12*, 301–347, doi:10.1016/S1387-2656(06)12009-8.
59. Mukherjee, C.; Varghese, D.; Krishna, J.S.; Boominathan, T.; Rakeshkumar, R.; Dineshkumar, S.; Brahmananda Rao, C.V.S.; Sivaramakrishna, A. Recent Advances in Biodegradable Polymers—Properties, Applications and Future Prospects. *Eur. Polym. J.* **2023**, *192*, 112068, doi:10.1016/j.eurpolymj.2023.112068.
60. Abizaid, A.; Ribamar Costa, J.J. Bioresorbable Scaffolds for Coronary Stenosis: When and How Based Upon Current Studies. *Curr. Cardiol. Rep.* **2017**, *19*, 27, doi:10.1007/s11886-017-0836-z.
61. Collet, C.; Asano, T.; Miyazaki, Y.; Tenekecioglu, E.; Katagiri, Y.; Sotomi, Y.; Cavalcante, R.; de Winter, R.J.; Kimura, T.; Gao, R.; et al. Late Thrombotic Events after Bioresorbable Scaffold Implantation: A Systematic Review and Meta-Analysis of Randomized Clinical Trials. *Eur. Heart J.* **2017**, *38*, 2559–2566, doi:10.1093/eurheartj/ehx155.
62. Arokiyasamy, D.A.; Tamilperuvalathan, S. A Comprehensive Evaluation of Material Properties, Degradation Kinetics and Clinical Performance of Biodegradable Polymer Cardiovascular Stents: A Review. *Int. J. Biol. Macromol.* **2026**, *343*, 150358, doi:10.1016/j.ijbiomac.2026.150358.
63. Kachel, M.; Melo, P.H.C.; Cheng, Y.; Conditt, G.B.; Gram, D.; Anderson, J.; Rousselle, S.D.; Parikh, S.A.; Granada, J.F.; Kaluza, G.L. The Preclinical Study of Biocompatibility of Tyrosine Polycarbonate Bioresorbable Scaffold in Small Caliber Porcine Peripheral Arteries. *Sci. Rep.* **2025**, *15*, 10624, doi:10.1038/s41598-025-91759-6.
64. Huang, Y.; Xu, Y.; Chen, X.; Armstrong, J.P.K.; Caputo, M.; Qi, Q.; Hicks, B.; Vyas, C.; Bartolo, P.; Biglino, G.; et al. 3D Printing of Biodegradable Polymer Vascular Stents to Treat Cardiovascular Diseases: A Review. *Addit. Manuf.* **2025**, *111*, 104984, doi:10.1016/j.addma.2025.104984.
65. Tarrahi, I.; Colombo, M.; Hartman, E.M.J.; Tovar Forero, M.N.; Torii, R.; Chiastra, C.; Daemen, J.; Gijsen, F.J.H. Impact of Bioresorbable Scaffold Design Characteristics on Local Haemodynamic Forces: An Ex Vivo Assessment with Computational Fluid Dynamics Simulations. *EuroIntervention* **2020**, *16*, e930–e937, doi:10.4244/EIJ-D-19-00657.
66. Kladovasilakis, N.; Kyriakidis, I.F.; Tzimtzimis, E.K.; Pechlivani, E.M.; Tsongas, K.; Tzetzis, D. Development of 4D-Printed Arterial Stents Utilizing Bioinspired Architected Auxetic Materials. *Biomimetics* **2025**, *10*, 78, doi:10.3390/biomimetics10020078.
67. Kalogeropoulou, M.; Díaz-Payno, P.J.; Mirzaali, M.J.; van Osch, G.J.V.M.; Fratila-Apachitei, L.E.; Zadpoor, A.A. 4D Printed Shape-Shifting Biomaterials for Tissue Engineering and Regenerative Medicine Applications. *Biofabrication* **2024**, *16*, doi:10.1088/1758-5090/ad1e6f.
68. Aussel, A.; Thébaud, N.B.; Bérard, X.; Brizzi, V.; Delmond, S.; Bareille, R.; Siadous, R.; James, C.; Ripoche, J.; Durand, M.; et al. Chitosan-Based Hydrogels for Developing a Small-Diameter Vascular Graft: In Vitro and in Vivo Evaluation. *Biomed. Mater. Bristol Engl.* **2017**, *12*, 065003, doi:10.1088/1748-605X/aa78d0.
69. Grabowski, M.; Gmyrek, D.; Żurawska, M.; Trusek, A. Biopolymers in Biotechnology and Tissue Engineering: A Comprehensive Review. *Macromol* **2025**, *5*, 34, doi:10.3390/macromol5030034.
70. Munoz-Pinto, D.J.; Guiza-Arguello, V.R.; Becerra-Bayona, S.M.; Erndt-Marino, J.; Samavedi, S.; Malmut, S.; Russell, B.; Höök, M.; Hahn, M.S. Collagen-Mimetic Hydrogels Promote Human Endothelial Cell Adhesion, Migration and Phenotypic Maturation. *J. Mater. Chem. B* **2015**, *3*, 7912–7919, doi:10.1039/C5TB00990A.
71. Wang, P.; Liu, J.; Zhang, T. In Vitro Biocompatibility of Electrospun Chitosan/Collagen Scaffold. *J. Nanomater.* **2013**, *2013*, 958172, doi:10.1155/2013/958172.
72. Yang, C.; Su, C.; Zou, J.; Zhong, B.; Wang, L.; Chen, B.; Li, J.; Wei, M. Investigating the Efficacy of Uncrosslinked Porcine Collagen Coated Vascular Grafts for Neointima Formation and Endothelialization. *Front. Bioeng. Biotechnol.* **2024**, *12*, 1418259, doi:10.3389/fbioe.2024.1418259.

 doi:10.20944/preprints202606.0497.v1

73. Abedini, E.; Feizlou, N. The Biomechanical Performance of Natural and Synthetic Polymers in Vascular Surgery: A Systematic Review. *Proceedings* **2026**, *136*, 82, doi:10.3390/proceedings2026136082.
74. Das, K.K.; Tiwari, R.M.; Shankar, O.; Maiti, P.; Dubey, A.K. Tissue-Engineered Vascular Grafts for Cardiovascular Disease Management: Current Strategies, Challenges, and Future Perspectives. *MEDCOMM—Biomater. Appl.* **2024**, *3*, 88–40.
75. Di Francesco, D.; Pigliafreddo, A.; Casarella, S.; Di Nunno, L.; Mantovani, D.; Boccafoschi, F. Biological Materials for Tissue-Engineered Vascular Grafts: Overview of Recent Advancements. *Biomolecules* **2023**, *13*, doi:10.3390/biom13091389.
76. Moore, M.J.; Tan, R.P.; Yang, N.; Rnjak-Kovacina, J.; Wise, S.G. Bioengineering Artificial Blood Vessels from Natural Materials. *Trends Biotechnol.* **2022**, *40*, 693–707, doi:10.1016/j.tibtech.2021.11.003.
77. Kang, M.-K.; Heo, S.-H.; Yoon, J.-K. In-Stent Re-Endothelialization Strategies: Cells, Extracellular Matrix, and Extracellular Vesicles. *Tissue Eng. Part B Rev.* **2025**, *31*, 317–330, doi:10.1089/ten.TEB.2024.0178.
78. Bi, S.; Lin, H.; Zhu, K.; Zhu, Z.; Zhang, W.; Yang, X.; Chen, S.; Zhao, J.; Liu, M.; Pan, P.; et al. Chitosan-Salvianolic Acid B Coating on the Surface of Nickel-Titanium Alloy Inhibits Proliferation of Smooth Muscle Cells and Promote Endothelialization. *Front. Bioeng. Biotechnol.* **2023**, *11*, 1300336, doi:10.3389/fbioe.2023.1300336.
79. Liang, M.; Zuo, D.; Wang, F.; Zhang, B.; Tian, J.; Huang, X.; Sun, Y.; Li, G.; Zhang, X.; Li, G. Drug-Eluting Vascular Stents with Surface Modification of Anticoagulation and pro-Endothelialization. *Biomacromolecules* **2025**, *26*, 7074–7084, doi:10.1021/acs.biomac.5c01382.
80. Durak, B.; Erdoğan, N.; Sen Karaman, D. Design and in Vitro Assessment of Curcumin-Eluting Bilayer Nanofiber Coatings for Improved Endothelialization and Blood Compatibility of Vascular Stents. *Acad. Mater. Sci.* **2025**, *2*, doi:10.20935/AcadMatSci8092.
81. Lee, C.-H.; Yu, C.-Y.; Chang, S.-H.; Hung, K.-C.; Liu, S.-J.; Wang, C.-J.; Hsu, M.-Y.; Hsieh, I.-C.; Chen, W.-J.; Ko, Y.-S.; et al. Promoting Endothelial Recovery and Reducing Neointimal Hyperplasia Using Sequential-like Release of Acetylsalicylic Acid and Paclitaxel-Loaded Biodegradable Stents. *Int. J. Nanomedicine* **2014**, *9*, 4117–4133, doi:10.2147/IJN.S67721.
82. Mukheja, Y.; Sarkar, A.; Arora, R.; Pal, K.; Ahuja, A.; Vashishth, A.; Kuhad, A.; Chopra, K.; Jain, M. Unravelling the Progress and Potential of Drug-Eluting Stents and Drug-Coated Balloons in Cardiological Insurgencies. *Life Sci.* **2024**, *352*, 122908, doi:10.1016/j.lfs.2024.122908.
83. Chen, Y.; Gao, P.; Huang, L.; Tan, X.; Zhou, N.; Yang, T.; Qiu, H.; Dai, X.; Michael, S.; Tu, Q.; et al. A Tough Nitric Oxide-Eluting Hydrogel Coating Suppresses Neointimal Hyperplasia on Vascular Stent. *Nat. Commun.* **2021**, *12*, doi:10.1038/s41467-021-27368-4.
84. Wang, R.; Lu, J.; Yin, J.; Chen, H.; Liu, H.; Xu, F.; Zang, T.; Xu, R.; Li, C.; Wu, Y.; et al. A TEMPOL and Rapamycin Loaded Nanofiber-Covered Stent Favors Endothelialization and Mitigates Neointimal Hyperplasia and Local Inflammation. *Bioact. Mater.* **2023**, *19*, 666–677, doi:10.1016/j.bioactmat.2022.04.033.
85. Zhang, B.; Qin, Y.; Yang, L.; Wu, Y.; Chen, N.; Li, M.; Li, Y.; Wan, H.; Fu, D.; Luo, R.; et al. A Polyphenol-Network-Mediated Coating Modulates Inflammation and Vascular Healing on Vascular Stents. *ACS Nano* **2022**, *16*, 6585–6597, doi:10.1021/acsnano.2c00642.
86. Tong, S.; Chen, J.; Li, Y.; Zhao, W. Emerging Gel Technologies for Atherosclerosis Research and Intervention. *GELS* **2026**, *12*, doi:10.3390/gels12010080.
87. Hou, J.; Zhang, X.; Wu, Y.; Jie, J.; Wang, Z.; Chen, G.-Q.; Sun, J.; Wu, L.-P. Amphiphilic and Fatigue-Resistant Organohydrogels for Small-Diameter Vascular Grafts. *Sci. Adv.* **2022**, *8*, eabn5360, doi:10.1126/sciadv.abn5360.
88. Zhao, Y.; Chen, C.; Zhu, Z.; Zhang, S.; Ma, X.; Shen, X.; Zhang, X.; Sun, Q.; Bi, H. Hofmeister Effect Driven Dynamic-Bond Cross-Linked Dialdehyde Xylan Hydrogels with Rapid Response and Robust Mechanical Properties for Expanding Stent. *Int. J. Biol. Macromol.* **2024**, *280*, 135888, doi:10.1016/j.ijbiomac.2024.135888.
89. Nakayama, Y.; Kim, J.; Nishi, S.; Ueno, H.; Matsuda, T. Development of High-Performance Stent: Gelatinous Photogel-Coated Stent That Permits Drug Delivery and Gene Transfer. *J. Biomed. Mater. Res.* **2001**, *57*, 559–566, doi:10.1002/1097-4636(20011215)57:4<559::AID-JBM1202>3.0.CO;2-H.

 doi:10.20944/preprints202606.0497.v1

90. Qiu, B.; Cheng, Q.; Chen, R.; Liu, C.; Qin, J.; Jiang, Q. Mussel-Mimetic Hydrogel Coating with Anticoagulant and Antiinflammatory Properties on a Poly(Lactic Acid) Vascular Stent. *BIOMACROMOLECULES* **2024**, *25*, 3098–3111, doi:10.1021/acs.biomac.4c00201.
91. Yang, F.; Guo, G.; Wang, Y. Inflammation-Directed Nanozyme-Eluting Hydrogel Coating Promotes Vascular Tissue Repair by Restoring Reactive Oxygen Species Homeostasis. *Chem. Eng. J.* **2023**, *454*, doi:10.1016/j.cej.2022.140556.
92. Wan, Z.; Li, D.; Zhou, Y.; Wang, T.; Zhu, B.; Du, C.; Li, Y.; Shu, C. Trials of a Drug Release Platform in Near-Spherical Porous NiTi Alloys Containing a Thermosensitive Hydrogel as the Inner Coating. *RSC Adv.* **2025**, *15*, 15639–15650, doi:10.1039/d5ra01925g.
93. Kim, J.; Ko, N.; Jung, B.; Kwon, I. Development of a Novel Dual PLGA and Alginate Coated Drug-Eluting Stent for Enhanced Blood Compatibility. *Macromol. Res.* **2016**, *24*, 931–939, doi:10.1007/s13233-016-4130-5.
94. Ebrahimi-Nozari, T.; Imani, R.; Haghbin-Nazarpak, M.; Nouri, A. Multimodal Effects of Asymmetric Coating of Coronary Stents by Electrospinning and Electrophoretic Deposition Br. *Int. J. Pharm.* **2023**, *630*, doi:10.1016/j.ijpharm.2022.122437.
95. Wei, L.; Lin, J.; Cai, C.; Fang, Z.; Fu, W. Drug-Carrier/Hydrogel Scaffold for Controlled Growth of Cells. *Eur. J. Pharm. Biopharm.* **2011**, *78*, 346–354, doi:10.1016/j.ejpb.2011.01.015.
96. Zhong, H.; Matsui, O.; Xu, K.; Ogi, T.; Sanada, J.; Okamoto, Y.; Tabata, Y.; Takuwa, Y. Gene Transduction into Aortic Wall Using Plasmid-Loaded Cationized Gelatin Hydrogel-Coated Polyester Stent Graft. *J. Vasc. Surg.* **2009**, *50*, 1433–1443, doi:10.1016/j.jvs.2009.07.071.
97. San Juan, A.; Bala, M.; Hlawaty, H.; Portes, P.; Vranckx, R.; Feldman, L.; Letourneur, D. Development of a Functionalized Polymer for Stent Coating in the Arterial Delivery of Small Interfering RNA. *BIOMACROMOLECULES* **2009**, *10*, 3074–3080, doi:10.1021/bm900740g.
98. Paul, A.; Shao, W.; Shum-Tim, D.; Prakash, S. The Attenuation of Restenosis Following Arterial Gene Transfer Using Carbon Nanotube Coated Stent Incorporating TAT/DNAAng1+Vegf Nanoparticles. *BIOMATERIALS* **2012**, *33*, 7655–7664, doi:10.1016/j.biomaterials.2012.06.096.
99. Zhang, J.; Li, Y.; Xiang, Z.; Fu, D.; Wang, Y. Spatiotemporally Orchestrated H2S/NO-Releasing Stent for Synergistic Vascular Healing. *Adv. Funct. Mater.* **2025**, doi:10.1002/adfm.202522266.
100. Wang, B.; Hua, J.; You, R.; Yan, K.; Ma, L. Electrochemically Deposition of Catechol-Chitosan Hydrogel Coating on Coronary Stent with Robust Copper Ions Immobilization Capability and Improved Interfacial Biological Activity. *Int. J. Biol. Macromol.* **2021**, *181*, 435–443, doi:10.1016/j.ijbiomac.2021.03.158.
101. Han, X.; Lu, B.; Zou, D.; Luo, X.; Liu, L.; Maitz, M.; Yang, P.; Huang, N.; Zhao, A.; Chen, J. Allicin-Loaded Intelligent Hydrogel Coating Improving Vascular Implant Performance. *ACS Appl. Mater. INTERFACES* **2023**, *15*, 38247–38263, doi:10.1021/acsami.3c05984.
102. Chen, N.; Li, M.; Wu, H.; Qin, Y.; Wang, J.; Xu, K.; Luo, R.; Yang, L.; Wang, Y.; Zhang, X. An Extracellular Matrix-Mimetic Coating with Dual Bionics for Cardiovascular Stents. *Regen. Biomater.* **2023**, *10*, doi:10.1093/rb/rbad055.
103. Rezvova, M.A.; Ovcharenko, E.A.; Klyshnikov, K.Y.; Glushkova, T.V.; Kostyunin, A.E.; Shishkova, D.K.; Matveeva, V.G.; Velikanova, E.A.; Shabaev, A.R.; Kudryavtseva, Y.A. Electrospun Bioresorbable Polymer Membranes for Coronary Artery Stents. *Front. Bioeng. Biotechnol.* **2024**, *12*, 1440181, doi:10.3389/fbioe.2024.1440181.
104. Wright, J.; Nguyen, A.; D'Souza, N.; Forbess, J.M.; Nugent, A.; Reddy, S.R.V.; Jaquiss, R.; Welch, T.R. Bioresorbable Stent to Manage Congenital Heart Defects in Children. *Materialia* **2021**, *16*, 101078, doi:10.1016/j.mtla.2021.101078.
105. Hataminia, F.; Faridi-Majidi, R.; Hashemi, S.M.A.; Ghanbari, H. Fabrication of a Multilayer Bioabsorbable Composite Vascular Stent Utilizing Oxidized Starch-Fe(3)O(4) Nanoparticles and Polycaprolactone Nanofibers. *Sci. Rep.* **2025**, *15*, 7454, doi:10.1038/s41598-025-86111-x.
106. Lin, M.; Lin, J.; Huang, C.; Chen, Y. Textile Fabricated Biodegradable Composite Stents with Core-Shell Structure. *Polym. Test.* **2020**, *81*, doi:10.1016/j.polymertesting.2019.106166.
107. Nazarkina, Z.; Chelobanov, B.; Kuznetsov, K.; Shutov, A.; Romanova, I.; Karpenko, A.; Laktionov, P. Influence of Elongation of Paclitaxel-Eluting Electrospun-Produced Stent Coating on Paclitaxel Release and Transport through the Arterial Wall after Stenting. *POLYMERS* **2021**, *13*, doi:10.3390/polym13071165.

 doi:10.20944/preprints202606.0497.v1

108. Wang, J.; An, Q.; Li, D.; Wu, T.; Chen, W.; Sun, B.; El-Hamshary, H.; Al-Deyab, S.; Zhu, W.; Mo, X. Heparin and Vascular Endothelial Growth Factor Loaded Poly(L-Lactide-Co-Caprolactone) Nanofiber Covered Stent-Graft for Aneurysm Treatment. *J. Biomed. Nanotechnol.* **2015**, *11*, 1947–1960, doi:10.1166/jbn.2015.2138.
109. Zhang, Y.; Wang, J.; Xiao, J.; Fang, T.; Hu, N.; Li, M.; Deng, L.; Cheng, Y.; Zhu, Y.; Cui, W. An Electrospun Fiber-Covered Stent with Programmable Dual Drug Release for Endothelialization Acceleration and Lumen Stenosis Prevention. *ACTA Biomater.* **2019**, *94*, 295–305, doi:10.1016/j.actbio.2019.06.008.
110. Flores, A.; Ye, J.; Jarr, K.; Hosseini-Nassab, N.; Smith, B.; Leeper, N. Nanoparticle Therapy for Vascular Diseases. *Arterioscler. Thromb. Vasc. Biol.* **2019**, *39*, 635–646, doi:10.1161/ATVBAHA.118.311569.
111. Zhao, L.; Feng, L.; Shan, R.; Huang, Y.; Shen, L.; Fan, M.; Wang, Y. Nanoparticle-Based Approaches for Treating Restenosis after Vascular Injury. *Front. Pharmacol.* **2024**, *15*, doi:10.3389/fphar.2024.1427651.
112. Che, H.; Bae, I.; Lim, K.; Song, I.; Lee, H.; Muthiah, M.; Namgung, R.; Kim, W.; Kim, D.; Ahn, Y.; et al. Suppression of Post-Angioplasty Restenosis with an Akt1 siRNA-Embedded Coronary Stent in a Rabbit Model. *BIOMATERIALS* **2012**, *33*, 8548–8556, doi:10.1016/j.biomaterials.2012.07.045.
113. Che, H.; Bae, I.; Lim, K.; Uthaman, S.; Song, I.; Lee, H.; Lee, D.; Kim, W.; Ahn, Y.; Park, I.; et al. Novel Fabrication of MicroRNA Nanoparticle-Coated Coronary Stent for Prevention of Post-Angioplasty Restenosis. *KOREAN Circ. J.* **2016**, *46*, 23–32, doi:10.4070/kcj.2016.46.1.23.
114. Chorny, M.; Fishbein, I.; Forbes, S.; Alferiev, I. Magnetic Nanoparticles for Targeted Vascular Delivery. *IUBMB LIFE* **2011**, *63*, 613–620, doi:10.1002/iub.479.
115. Nakano, K.; Egashira, K.; Masuda, S.; Funakoshi, K.; Zhao, G.; Kimura, S.; Matoba, T.; Sueishi, K.; Endo, Y.; Kawashima, Y.; et al. Formulation of Nanoparticle-Eluting Stents by a Cationic Electrodeposition Coating Technology Efficient Nano-Drug Delivery via Bioabsorbable Polymeric Nanoparticle-Eluting Stents in Porcine Coronary Arteries. *JACC-Cardiovasc. Interv.* **2009**, *2*, 277–283, doi:10.1016/j.jcin.2008.08.023.
116. Zago, A.; Raudales, J.; Attizzani, G.; Matte, B.; Yamamoto, G.; Balvedi, J.; Nascimento, L.; Kosachenco, B.; Centeno, P.; Zago, A. Local Delivery of Sirolimus Nanoparticles for the Treatment of In-Stent Restenosis. *Catheter. Cardiovasc. Interv.* **2013**, *81*, E124–E129, doi:10.1002/ccd.24331.
117. Tsukie, N.; Nakano, K.; Matoba, T.; Masuda, S.; Iwata, E.; Miyagawa, M.; Zhao, G.; Meng, W.; Kishimoto, J.; Sunagawa, K.; et al. Pitavastatin-Incorporated Nanoparticle-Eluting Stents Attenuate In-Stent Stenosis without Delayed Endothelial Healing Effects in a Porcine Coronary Artery Model. *J. Atheroscler. Thromb.* **2013**, *20*, 32–45, doi:10.5551/jat.13862.
118. Chorny, M.; Fishbein, I.; Yellen, B.; Alferiev, I.; Bakay, M.; Ganta, S.; Adamo, R.; Amiji, M.; Friedman, G.; Levy, R. Targeting Stents with Local Delivery of Paclitaxel-Loaded Magnetic Nanoparticles Using Uniform Fields. *Proc. Natl. Acad. Sci. U. S. A.* **2010**, *107*, 8346–8351, doi:10.1073/pnas.0909506107.
119. Zhao, Y.; Shirasu, T.; Yodsanit, N.; Kent, E.; Ye, M.; Wang, Y.; Xie, R.; Gregg, A.; Huang, Y.; Kent, K.; et al. Biomimetic, ROS-Detonable Nanoclusters-A Multimodal Nanoplatform for Anti-Restenotic Therapy. *J. Controlled Release* **2021**, *338*, 295–306, doi:10.1016/j.jconrel.2021.08.025.
120. Che, H.; Bae, I.; Lim, K.; Song, I.; Lee, H.; Lee, D.; Kim, W.; Jeong, M.; Park, I.; Ahn, Y. Therapeutic Effect of Akt1 siRNA Nanoparticle Eluting Coronary Stent on Suppression of Post-Angioplasty Restenosis. *J. Biomed. Nanotechnol.* **2016**, *12*, 1211–1222, doi:10.1166/jbn.2016.2255.
121. Izuhara, M.; Kuwabara, Y.; Saito, N.; Yamamoto, E.; Hakuno, D.; Nakashima, Y.; Horie, T.; Baba, O.; Nishiga, M.; Nakao, T.; et al. Prevention of Neointimal Formation Using miRNA-126-Containing Nanoparticle-Conjugated Stents in a Rabbit Model. *PLOS ONE* **2017**, *12*, doi:10.1371/journal.pone.0172798.
122. Wang, Y.; Li, M.; Sheng, Z.; Ran, H.; Dong, J.; Fang, L.; Zhang, P. Ultrasound-Mediated Delivery of Pik3cb shRNA Using Magnetic Nanoparticles for the Treatment of in-Stent Restenosis in a Rat Balloon-Injured Model. *J. Radiat. Res. (Tokyo)* **2024**, *65*, 47–54, doi:10.1093/jrr/rrad083.
123. Luo, R.; Zhang, J.; Zhuang, W.; Deng, L.; Li, L.; Yu, H.; Wang, J.; Huang, N.; Wang, Y. Multifunctional Coatings That Mimic the Endothelium: Surface Bound Active Heparin Nanoparticles with in Situ Generation of Nitric Oxide from Nitrosothiols. *J. Mater. Chem. B* **2018**, *6*, 5582–5595, doi:10.1039/c8tb00596f.
124. Li, Y.; Zhang, B.; Liu, X.; Wan, H.; Qin, Y.; Yan, H.; Wang, Y.; An, Y.; Yang, Y.; Dai, Y.; et al. A Bio-Inspired Nanoparticle Coating for Vascular Healing and Immunomodulatory by cGMP-PKG and NF-Kappa B Signaling Pathways. *BIOMATERIALS* **2023**, *302*, doi:10.1016/j.biomaterials.2023.122288.

 doi:10.20944/preprints202606.0497.v1

125. Hou, Y.; Li, J.; Cao, C.; Su, C.; Qin, Z.; Zhang, G.; Guo, J.; Tang, J.; Zhang, J.; Guan, S. Biodegradable Mg Alloy Modified with Bioactive Exosomes for Cardiovascular Stent Application. *J. Magnes. ALLOYS* **2024**, *12*, 4988–5004, doi:10.1016/j.jma.2023.05.007.
126. Polyak, B.; Medved, M.; Lazareva, N.; Steele, L.; Patel, T.; Rai, A.; Rotenberg, M.; Wasko, K.; Kohut, A.; Sensenig, R.; et al. Magnetic Nanoparticle-Mediated Targeting of Cell Therapy Reduces In-Stent Stenosis in Injured Arteries. *ACS NANO* **2016**, *10*, 9559–9569, doi:10.1021/acsnano.6b04912.
127. Arai, D.; Ishii, A.; Ikeda, H.; Abekura, Y.; Nishi, H.; Miyamoto, S.; Tabata, Y. Development of a Stent Capable of the Controlled Release of Basic Fibroblast Growth Factor and Argatroban to Treat Cerebral Aneurysms: In Vitro Experiment and Evaluation in a Rabbit Aneurysm Model. *J. Biomed. Mater. Res. B Appl. Biomater.* **2019**, *107*, 2185–2194, doi:10.1002/jbm.b.34314.
128. Indolfi, L.; Causa, F.; Giovino, C.; Ungaro, F.; Quaglia, F.; Netti, P.A. Microsphere-Integrated Drug-Eluting Stents: PLGA Microsphere Integration in Hydrogel Coating for Local and Prolonged Delivery of Hydrophilic Antirestenosis Agents. *J. Biomed. Mater. Res. A* **2011**, *97*, 201–211, doi:10.1002/jbm.a.33039.
129. Liang, M.; Li, F.; Wang, Y.; Chen, H.; Tian, J.; Zhao, Z.; Schneider, K.H.; Li, G. Woven Vascular Stent-Grafts with Surface Modification of Silk Fibroin-Based Paclitaxel/Metformin Microspheres. *Bioeng. Basel Switz.* **2023**, *10*, doi:10.3390/bioengineering10040399.
130. Do, Y.; Kao, E.; Ganaha, F.; Minamiguchi, H.; Sugimoto, K.; Lee, J.; Elkins, C.; Amabile, P.; Kuo, M.; Wang, D.; et al. In-Stent Restenosis Limitation with Stent-Based Controlled-Release Nitric Oxide: Initial Results in Rabbits. *RADIOLOGY* **2004**, *230*, 377–382, doi:10.1148/radiol.2302020417.
131. Li, M.; Wu, H.; Wang, Y.; Yin, T.; Gregersen, H.; Zhang, X.; Liao, X.; Wang, G. Immobilization of Heparin/Poly-L-Lysine Microspheres on Medical Grade High Nitrogen Nickel-Free Austenitic Stainless Steel Surface to Improve the Biocompatibility and Suppress Thrombosis. *Mater. Sci. Eng. C-Mater. Biol. Appl.* **2017**, *73*, 198–205, doi:10.1016/j.msec.2016.12.070.
132. Pislaru, S.; Harbuzariu, A.; Gulati, R.; Witt, T.; Sandhu, N.; Simari, R.; Sandhu, G. Magnetically Targeted Endothelial Cell Localization in Stented Vessels. *J. Am. Coll. Cardiol.* **2006**, *48*, 1839–1845, doi:10.1016/j.jacc.2006.06.069.
133. Nonn, A.; Kirschner, S.; Figueiredo, G.; Kramer, M.; Nikoubashman, O.; Pjontek, R.; Wiesmann, M.; Brockmann, M.A. Feasibility, Safety, and Efficacy of Flow-Diverting Stent-Assisted Microsphere Embolization of Fusiform and Sidewall Aneurysms. *Neurosurgery* **2015**, *77*, 126–135; discussion 135-136, doi:10.1227/NEU.0000000000000687.
134. Gutman, D.; Golomb, G. Liposomal Alendronate for the Treatment of Restenosis. *Drug Deliv. Res. Eur.* **2012**, *161*, 619–627, doi:10.1016/j.jconrel.2011.11.037.
135. Haeri, A.; Osouli, M.; Bayat, F.; Alavi, S.; Dadashzadeh, S. Nanomedicine Approaches for Sirolimus Delivery: A Review of Pharmaceutical Properties and Preclinical Studies. *Artif. Cells Nanomedicine Biotechnol.* **2018**, *46*, 1–14, doi:10.1080/21691401.2017.1408123.
136. Brito, L.A.; Chandrasekhar, S.; Little, S.R.; Amiji, M.M. In Vitro and in Vivo Studies of Local Arterial Gene Delivery and Transfection Using Lipopolyplexes-Embedded Stents. *J. Biomed. Mater. Res. A* **2010**, *93*, 325–336, doi:10.1002/jbm.a.32488.
137. Sharif, F.; Hynes, S.O.; McCullagh, K.J.A.; Ganley, S.; Greiser, U.; McHugh, P.; Crowley, J.; Barry, F.; O'Brien, T. Gene-Eluting Stents: Non-Viral, Liposome-Based Gene Delivery of eNOS to the Blood Vessel Wall in Vivo Results in Enhanced Endothelialization but Does Not Reduce Restenosis in a Hypercholesterolemic Model. *Gene Ther.* **2012**, *19*, 321–328, doi:10.1038/gt.2011.92.
138. Jun, H.; Cross, R.; Zhang, X.; Chen, J.; Ahn, Y.; Brott, B.; Anderson, P.; Sherwood, J.; Yoon, Y.; Virmani, R. Abstract 4124070: Dual-Action Nanomatrix Coated Stent for Improving Endothelialization While Suppressing Restenosis and Inflammation. *Circulation* **2024**, *150*, A4124070–A4124070, doi:10.1161/circ.150.suppl_1.4124070.
139. Vučemilović, A. Exosomes: Intriguing Mediators of Intercellular Communication in the Organism's Response to Noxious Agents. *Arch. Ind. Hyg. Toxicol.* **2024**, *75*, 228–239, doi:10.2478/aiht-2024-75-3923.
140. Wang, X.; Liu, Y.; Li, W.; Hao, J.; Zhao, Z.; Fan, H.; Wu, X.; Liu, X.; Xu, H.; Yu, T.; et al. Coptis Chinensis Extracellular Vesicles Loaded with CA1-siRNA Promote Endothelial Repair and Stent Restenosis Therapy

 doi:10.20944/preprints202606.0497.v1

by Regulating the PADI2 and NF-κB Pathway. *J. Nanobiotechnology* **2026**, *24*, 157, doi:10.1186/s12951-026-04092-z.

141. Hu, S.; Li, Z.; Shen, D.; Zhu, D.; Huang, K.; Su, T.; Dinh, P.-U.; Cores, J.; Cheng, K. Exosome-Eluting Stents for Vascular Healing after Ischaemic Injury. *Nat. Biomed. Eng.* **2021**, *5*, 1174–1188, doi:10.1038/s41551-021-00705-0.
142. Fishbein, I.; Guerrero, D.T.; Alferiev, I.S.; Foster, J.B.; Minutolo, N.G.; Chorny, M.; Monteys, A.M.; Driesbaugh, K.H.; Nagaswami, C.; Levy, R.J. Stent-Based Delivery of Adeno-Associated Viral Vectors with Sustained Vascular Transduction and iNOS-Mediated Inhibition of in-Stent Restenosis. *Gene Ther.* **2017**, *24*, 717–726, doi:10.1038/gt.2017.82.
143. Alferiev, I.S.; Chorny, M.; Wilensky, R.L.; Levy, R.J.; Fishbein, I. Stent-Based Gene Delivery for Coronary Disease. *Methods Mol. Biol. Clifton NJ* **2022**, *2573*, 217–233, doi:10.1007/978-1-0716-2707-5_17.
144. Hytönen, J.P.; Pajula, J.; Halonen, P.; Taavitsainen, J.; Kuivanen, A.; Tarvainen, S.; Heikkilä, M.; Mäkinen, P.; Koistinen, A.; Laakkonen, J.P.; et al. Endothelialization of Coronary Stents after Intra-Luminal Adenoviral VEGF-A Gene Transfer in a Preclinical Porcine Restenosis Model—Studies with Optical Coherence Tomography, Angioscopy, Multiphoton and Scanning Electron Microscopy. *J. Mol. Cell. Cardiol.* **2025**, *199*, 118–125, doi:10.1016/j.yjmcc.2024.12.007.
145. Kumar, A.; Bhatnagar, N. Finite Element Simulation and Testing of Cobalt-Chromium Stent: A Parametric Study on Radial Strength, Recoil, Foreshortening, and Dogboning. *Comput. Methods Biomech. Biomed. Engin.* **2021**, *24*, 245–259, doi:10.1080/10255842.2020.1822823.
146. Fan, Z.; Lu, J.; Cheng, H.; Ye, X.; Deng, X.; Zhao, P.; Liu, J.; Liu, M. Insights from Computational Fluid Dynamics and In Vitro Studies for Stent Protrusion in Iliac Vein: How Far Shall We Go? *Cardiovasc. Eng. Technol.* **2025**, *16*, 79–90, doi:10.1007/s13239-024-00758-7.
147. Gupta, K.; Meena, K.; Bhatnagar, N. Design, Development and Manufacturing of Re-Entrant Auxetic Stent Implant for Enhanced Mechanical Attributes. *Thin-Walled Struct.* **2026**, *219*, 114309, doi:10.1016/j.tws.2025.114309.
148. Dangas, G.; Peters-Veluthamaningal, C.; Cocke, T.P.; Vidhun, R.; Duvvuri, S.; Marmur, J.D.; Sharma, S.K. Histopathological Correlates of Early Arterial Recoil Following Directional Coronary Atherectomy. *Cardiology* **1998**, *90*, 32–36, doi:10.1159/000006813.
149. Yerra, S.; Kishore Y, R. Case Report: Case of Coronary Stent Longitudinal Deformation. *Indian J. Cardiovasc. Dis. Women WINCARS* **2019**, *04*, doi:10.1055/s-0039-3399617.
150. Pan, C.; Zeng, X.; Han, Y.; Lu, J. Investigation of Braided Stents in Curved Vessels in Terms of "Dogbone" Deformation. *Math. Biosci. Eng. MBE* **2022**, *19*, 5717–5737, doi:10.3934/mbe.2022267.
151. Obermaier, L.; Lehle, K.; Schmid, S.; Schmid, C.; Schratzenstaller, T. Introduction of a New Ex Vivo Porcine Coronary Artery Model: Evaluation of the Direct Vascular Injury after Stent Implantation with and without Dogbone Effect. *Eur. Surg. Res. Eur. Chir. Forsch. Rech. Chir. Eur.* **2022**, *63*, 285–293, doi:10.1159/000527883.
152. Hehrlein, C.; DeVries, J.J.; Arab, A.; Haller, S.D.; Kloostra, A.; Lauer, M.A.; Foster, M.T.; Fischell, T.A. Role of the "Dogbone" Effect of Balloon-Expandable Stents: Quantitative Coronary Analysis of DUET and NIR Stent Implantation Introducing a Novel Indexing System. *J. Invasive Cardiol.* **2002**, *14*, 59–65.
153. Abbaslou, M.; Hashemi, R.; Etemadi, E. Novel Hybrid 3D-Printed Auxetic Vascular Stent Based on Re-Entrant and Meta-Trichiral Unit Cells: Finite Element Simulation with Experimental Verifications. *Mater. Today Commun.* **2023**, *35*, 105742, doi:10.1016/j.mtcomm.2023.105742.
154. Watson, T.; Webster, M.W.I.; Ormiston, J.A.; Ruygrok, P.N.; Stewart, J.T. Long and Short of Optimal Stent Design. *Open Heart* **2017**, *4*, e000680, doi:10.1136/openhrt-2017-000680.
155. Carbonaro, D.; Ferro, N.; Mezzadri, F.; Gallo, D.; Audenino, A.L.; Perotto, S.; Morbiducci, U.; Chiastra, C. Easy-to-Use Formulations Based on the Homogenization Theory for Vascular Stent Design and Mechanical Characterization. *Comput. Methods Programs Biomed.* **2024**, *257*, 108467, doi:10.1016/j.cmpb.2024.108467.
156. Li, Y.; Wang, Y.; Shen, Z.; Miao, F.; Wang, J.; Sun, Y.; Zhu, S.; Zheng, Y.; Guan, S. A Biodegradable Magnesium Alloy Vascular Stent Structure: Design, Optimisation and Evaluation. *Acta Biomater.* **2022**, *142*, 402–412, doi:10.1016/j.actbio.2022.01.045.

 doi:10.20944/preprints202606.0497.v1

157. Xia, Y.; Han, Y.; Pan, C.; Lu, J.; Tang, S.; Fan, H.; Wang, H.; Xiang, Z.; Gong, C.; Wang, R. Design of M-Shaped Bistable Structure and Its Application on High Radial Strength Polymer Stent. *Results Eng.* **2025**, *26*, 104829, doi:10.1016/j.rineng.2025.104829.
158. Wei, Y.; Wang, M.; Zhao, D.; Li, H.; Jin, Y. Structural Design of Mechanical Property for Biodegradable Polymeric Stent. *Adv. Mater. Sci. Eng.* **2019**, *2019*, 2960435, doi:10.1155/2019/2960435.
159. Wang, H.; Jiao, L.; Sun, J.; Yan, P.; Wang, X.; Qiu, T. Multi-Objective Optimization of Bioresorbable Magnesium Alloy Stent by Kriging Surrogate Model. *Cardiovasc. Eng. Technol.* **2022**, *13*, 829–839, doi:10.1007/s13239-022-00619-1.
160. Hasanzadeh, R.; Jolaiy, S.; Mojaver, M.; Azdast, T.; Park, C.B. Auxetic 3D Printed Metastructure Stents for Enhanced Mechanical and Structural Performance and Biocompatibility in Coronary Artery Treatments. *Acta Biomater.* **2025**, *202*, 641–659, doi:10.1016/j.actbio.2025.06.043.
161. Zhang, A.; Fan, X.; Yang, Z.; Xie, Y.; Wu, T.; Zhang, M.; Xue, Y.; Wang, Y.; Zhao, Y.; Wu, X.; et al. Optimized Design and Biomechanical Evaluation of Biodegradable Magnesium Alloy Vascular Stents. *Acta Mech. Sin.* **2024**, *41*, 624055, doi:10.1007/s10409-024-24055-x.
162. Cui, F.; Lee, H.; Lu, C.; Chai, P. Effects of Balloon Length and Compliance on Vascular Stent Expansion. *Int. J. Appl. Mech.* **2010**, *2*, 681–697, doi:10.1142/S1758825110000718.
163. Murphy, J.; Boyle, F. Predicting Neointimal Hyperplasia in Stented Arteries Using Time-Dependant Computational Fluid Dynamics: A Review. *Comput. Biol. Med.* **2010**, *40*, 408–418, doi:10.1016/j.compbiomed.2010.02.005.
164. Cheng, C.K.; Wang, N.; Wang, L.; Huang, Y. Biophysical and Biochemical Roles of Shear Stress on Endothelium: A Revisit and New Insights. *Circ. Res.* **2025**, *136*, 752–772, doi:10.1161/CIRCRESAHA.124.325685.
165. Ng, J.; Bourantas, C.V.; Torii, R.; Ang, H.Y.; Tenekecioglu, E.; Serruys, P.W.; Foin, N. Local Hemodynamic Forces After Stenting: Implications on Restenosis and Thrombosis. *Arterioscler. Thromb. Vasc. Biol.* **2017**, *37*, 2231–2242, doi:10.1161/ATVBAHA.117.309728.
166. Chen, W.X.; Poon, E.K.W.; Hutchins, N.; Thondapu, V.; Barlis, P.; Ooi, A. Computational Fluid Dynamics Study of Common Stent Models inside Idealised Curved Coronary Arteries. *Comput. Methods Biomech. Biomed. Engin.* **2017**, *20*, 671–681, doi:10.1080/10255842.2017.1289374.
167. Poon, E.K.W.; Barlis, P.; Moore, S.; Pan, W.-H.; Liu, Y.; Ye, Y.; Xue, Y.; Zhu, S.J.; Ooi, A.S.H. Numerical Investigations of the Haemodynamic Changes Associated with Stent Malapposition in an Idealised Coronary Artery. *J. Biomech.* **2014**, *47*, 2843–2851, doi:10.1016/j.jbiomech.2014.07.030.
168. Wang, H.; Balzani, D.; Vedula, V.; Uhlmann, K.; Varnik, F. On the Potential Self-Amplification of Aneurysms Due to Tissue Degradation and Blood Flow Revealed From FSI Simulations. *Front. Physiol.* **2021**, *12*, 785780, doi:10.3389/fphys.2021.785780.
169. Elliott, M.; Cole, J.; Blair, R.; Menary, G. Highlighting Hemodynamic Risks for Bioresorbable Stents in Coronary Arteries. *FLUIDS* **2023**, *8*, doi:10.3390/fluids8090241.
170. Pant, S.; Bressloff, N.W.; Forrester, A.I.J.; Curzen, N. The Influence of Strut-Connectors in Stented Vessels: A Comparison of Pulsatile Flow through Five Coronary Stents. *Ann. Biomed. Eng.* **2010**, *38*, 1893–1907, doi:10.1007/s10439-010-9962-0.
171. Kandangwa, P.; Cheng, K.; Patel, M.; Sherwin, S.J.; de Silva, R.; Weinberg, P.D. Relative Residence Time Can Account for Half of the Anatomical Variation in Fatty Streak Prevalence Within the Right Coronary Artery. *Ann. Biomed. Eng.* **2025**, *53*, 144–157, doi:10.1007/s10439-024-03607-9.
172. Lagache, M.; Coppel, R.; Finet, G.; Derimay, F.; Pettigrew, R.I.; Ohayon, J.; Malvè, M. Impact of Malapposed and Overlapping Stents on Hemodynamics: A 2D Parametric Computational Fluid Dynamics Study. *Mathematics* **2021**, *9*, 795, doi:10.3390/math9080795.
173. Arzani, A.; Gambaruto, A.M.; Chen, G.; Shadden, S.C. Wall Shear Stress Exposure Time: A Lagrangian Measure of near-Wall Stagnation and Concentration in Cardiovascular Flows. *Biomech. Model. Mechanobiol.* **2017**, *16*, 787–803, doi:10.1007/s10237-016-0853-7.
174. Trenti, C.; Ziegler, M.; Bjarnegård, N.; Ebbers, T.; Lindenberger, M.; Dyverfeldt, P. Wall Shear Stress and Relative Residence Time as Potential Risk Factors for Abdominal Aortic Aneurysms in Males: A 4D Flow

 doi:10.20944/preprints202606.0497.v1

Cardiovascular Magnetic Resonance Case-Control Study. *J. Cardiovasc. Magn. Reson. Off. J. Soc. Cardiovasc. Magn. Reson.* **2022**, *24*, 18, doi:10.1186/s12968-022-00848-2.

175. Chen, W.X.; Poon, E.K.W.; Thondapu, V.; Hutchins, N.; Barlis, P.; Ooi, A. Haemodynamic Effects of Incomplete Stent Apposition in Curved Coronary Arteries. *J. Biomech.* **2017**, *63*, 164–173, doi:10.1016/j.jbiomech.2017.09.016.
176. Beier, S.; Ormiston, J.; Webster, M.; Cater, J.; Norris, S.; Medrano-Gracia, P.; Young, A.; Cowan, B. Hemodynamics in Idealized Stented Coronary Arteries: Important Stent Design Considerations. *Ann. Biomed. Eng.* **2016**, *44*, 315–329, doi:10.1007/s10439-015-1387-3.
177. Jiang, Y.; Zhang, J.; Zhao, W. Influence of Strut Cross-Section of Stents on Local Hemodynamics in Stented Arteries. *Chin. J. Mech. Eng.* **2016**, *29*, 624–632, doi:10.3901/CJME.2016.0125.013.
178. Valentim, M.X.G.; Zinani, F.S.F.; da Fonseca, C.E.; Wermuth, D.P. Systematic Review on the Application of Computational Fluid Dynamics as a Tool for the Design of Coronary Artery Stents. *Beni-Suef Univ. J. Basic Appl. Sci.* **2023**, *12*, 49, doi:10.1186/s43088-023-00382-9.
179. Johari, N.; Hamady, M.; Xu, X. A Computational Study of the Effect of Stent Design on Local Hemodynamic Factors at the Carotid Artery Bifurcation. *ARTERY Res.* **2020**, *26*, 161–169, doi:10.2991/artres.k.200603.001.
180. Nada, A.; Hassan, M.A.; Fakhr, M.A.; El-Wakad, M.T.I. Studying the Effect of Stent Thickness and Porosity on Post-Stent Implantation Hemodynamics. *J. Med. Eng. Technol.* **2021**, *45*, 408–416, doi:10.1080/03091902.2021.1912204.
181. Balossino, R.; Gervaso, F.; Migliavacca, F.; Dubini, G. Effects of Different Stent Designs on Local Hemodynamics in Stented Arteries. *J. Biomech.* **2008**, *41*, 1053–1061, doi:10.1016/j.jbiomech.2007.12.005.
182. Martin, D.; Boyle, F. Sequential Structural and Fluid Dynamics Analysis of Balloon-Expandable Coronary Stents: A Multivariable Statistical Analysis. *Cardiovasc. Eng. Technol.* **2015**, *6*, 314–328, doi:10.1007/s13239-015-0219-9.
183. Chiastra, C.; Morlacchi, S.; Gallo, D.; Morbiducci, U.; Cárdenes, R.; Larrabide, I.; Migliavacca, F. Computational Fluid Dynamic Simulations of Image-Based Stented Coronary Bifurcation Models. *J. R. Soc. Interface* **2013**, *10*, 20130193, doi:10.1098/rsif.2013.0193.
184. Supraba, W.; Husni, P.; Hazrina, A.; Kusuma Dewi, M.; Yohana Chaerunisaa, A. Challenges and Strategies in Nanoparticle-Mediated Drug Release: Mechanisms and Future Directions. *Trends Sci.* **2025**, *22*, 10344, doi:10.48048/tis.2025.10344.
185. Raval, A.; Parikh, J.; ENGINEER, C. Mechanism and in Vitro Release Kinetic Study of Sirolimus from a Biodegradable Polymeric Matrix Coated Cardiovascular Stent. *Ind. Eng. Chem. Res.* **2011**, *50*, 9539–9549.
186. Zhao, H.Q.; Jayasinghe, D.; Hossainy, S.; Schwartz, L.B. A Theoretical Model to Characterize the Drug Release Behavior of Drug-Eluting Stents with Durable Polymer Matrix Coating. *J. Biomed. Mater. Res. A* **2012**, *100*, 120–124, doi:10.1002/jbm.a.33246.
187. McGinty, S.; McKee, S.; McCormick, C.; Wheel, M. Release Mechanism and Parameter Estimation in Drug-Eluting Stent Systems: Analytical Solutions of Drug Release and Tissue Transport. *Math. Med. Biol. J. IMA* **2015**, *32*, 163–186, doi:10.1093/imammb/dqt025.
188. Formaggia, L.; Minisini, S.; Zunino, P. Modeling Polymeric Controlled Drug Release and Transport Phenomena in the Arterial Tissue. *Math. Models Methods Appl. Sci.* **2010**, *20*, 1759–1786, doi:10.1142/S0218202510004787.
189. Zhu, X.; Braatz, R.D. A Mechanistic Model for Drug Release in PLGA Biodegradable Stent Coatings Coupled with Polymer Degradation and Erosion. *J. Biomed. Mater. Res. A* **2015**, *103*, 2269–2279, doi:10.1002/jbm.a.35357.
190. Naghipoor, J.; Ferreira, J.; de Oliveira, P.; Rabczuk, T. Tuning Polymeric and Drug Properties in a Drug Eluting Stent: A Numerical Study. *Appl. Math. Model.* **2016**, *40*, 8067–8086, doi:10.1016/j.apm.2016.04.001.
191. Gagliardi, M. Numerical Analysis of Paclitaxel-Eluting Coronary Stents: Mechanics and Drug Release Properties. *Med. Eng. Phys.* **2020**, *82*, 78–85, doi:10.1016/j.medengphy.2020.06.004.
192. Mongrain, R.; Faik, I.; Leask, R.L.; Rodés-Cabau, J.; Larose, E.; Bertrand, O.F. Effects of Diffusion Coefficients and Struts Apposition Using Numerical Simulations for Drug Eluting Coronary Stents. *J. Biomech. Eng.* **2007**, *129*, 733–742, doi:10.1115/1.2768381.

 doi:10.20944/preprints202606.0497.v1

193. Pontrelli, G.; de Monte, F. Mass Diffusion through Two-Layer Porous Media: An Application to the Drug-Eluting Stent. *Int. J. Heat Mass Transf.* **2007**, *50*, 3658–3669, doi:10.1016/j.ijheatmasstransfer.2006.11.003.
194. Pontrelli, G.; de Monte, F. A Multi-Layer Porous Wall Model for Coronary Drug-Eluting Stents. *Int. J. HEAT MASS Transf.* **2010**, *53*, 3629–3637, doi:10.1016/j.ijheatmasstransfer.2010.03.031.
195. Balakrishnan, B.; Tzafriri, A.R.; Seifert, P.; Groothuis, A.; Rogers, C.; Edelman, E.R. Strut Position, Blood Flow, and Drug Deposition: Implications for Single and Overlapping Drug-Eluting Stents. *Circulation* **2005**, *111*, 2958–2965, doi:10.1161/CIRCULATIONAHA.104.512475.
196. Hwang, C.W.; Wu, D.; Edelman, E.R. Physiological Transport Forces Govern Drug Distribution for Stent-Based Delivery. *Circulation* **2001**, *104*, 600–605, doi:10.1161/hc3101.092214.
197. Vairo, G.; Cioffi, M.; Cottone, R.; Dubini, G.; Migliavacca, F. Drug Release from Coronary Eluting Stents: A Multidomain Approach. *J. Biomech.* **2010**, *43*, 1580–1589, doi:10.1016/j.jbiomech.2010.01.033.
198. O'Brien, C.C.; Kolachalama, V.B.; Barber, T.J.; Simmons, A.; Edelman, E.R. Impact of Flow Pulsatility on Arterial Drug Distribution in Stent-Based Therapy. *J. Control. Release Off. J. Control. Release Soc.* **2013**, *168*, 115–124, doi:10.1016/j.jconrel.2013.03.014.
199. Bozsak, F.; Chomaz, J.-M.; Barakat, A.I. Modeling the Transport of Drugs Eluted from Stents: Physical Phenomena Driving Drug Distribution in the Arterial Wall. *Biomech. Model. Mechanobiol.* **2014**, *13*, 327–347, doi:10.1007/s10237-013-0546-4.
200. Borghi, A.; Foa, E.; Balossino, R.; Migliavacca, F.; Dubini, G. Modelling Drug Elution from Stents: Effects of Reversible Binding in the Vascular Wall and Degradable Polymeric Matrix. *Comput. Methods Biomech. Biomed. Engin.* **2008**, *11*, 367–377, doi:10.1080/10255840801887555.
201. McGinty, S.; Pontrelli, G. On the Role of Specific Drug Binding in Modelling Arterial Eluting Stents. *J. Math. Chem.* **2016**, *54*, 967–976, doi:10.1007/s10910-016-0618-7.
202. Tzafriri, A.R.; Levin, A.D.; Edelman, E.R. Diffusion-Limited Binding Explains Binary Dose Response for Local Arterial and Tumour Drug Delivery. *Cell Prolif.* **2009**, *42*, 348–363, doi:10.1111/j.1365-2184.2009.00602.x.
203. Saha, R.; Choudhury, S.; Mandal, A. Computational Simulation and Modelling of Arterial Drug Delivery From Half-Embedded Drug-Eluting Stents in Single-Layered Homogeneous Vessel Wall. *Commun. Math. Appl.* **2024**, *15*, 203–219, doi:10.26713/cma.v15i1.2373.
204. Mandal, A.P.; Mandal, P.K. Specific and Nonspecific Binding of Drug Eluted from a Half-Embedded Stent in Presence of Atherosclerotic Plaque. *Comput. Methods Biomech. Biomed. Engin.* **2022**, *25*, 922–935, doi:10.1080/10255842.2021.1986813.
205. Wang, S.; Zhou, Y.; Tan, J.; Xu, J.; Yang, J.; Liu, Y. Computational Modeling of Magnetic Nanoparticle Targeting to Stent Surface under High Gradient Field. *Comput. Mech.* **2014**, *53*, 403–412, doi:10.1007/s00466-013-0968-y.
206. Sarifuddin; Alsemiry, R.; Mandal, P. Effects of Coating Properties on Controlled Delivery from an Embedded Drug-Eluting Stent: A Simulation Study. *J. Biol. Syst.* **2021**, *29*, 687–717, doi:10.1142/S0218339021500145.
207. Sarifuddin; Roy, S.; Mandal, P.K. Computational Model of Stent-Based Delivery from a Half-Embedded Two-Layered Coating. *Comput. Methods Biomech. Biomed. Engin.* **2020**, *23*, 815–831, doi:10.1080/10255842.2020.1767775.
208. Pontrelli, G.; Di Mascio, A.; De Monte, F. Local Mass Non-Equilibrium Dynamics in Multi-Layered Porous Media: Application to the Drug-Eluting Stent. *Int. J. HEAT MASS Transf.* **2013**, *66*, 844–854, doi:10.1016/j.ijheatmasstransfer.2013.07.041.
209. Chen, Y.; Jiang, W.; Chen, X.; Zheng, T.; Wang, Q.; Fan, Y. Numerical Simulation on Effects of Drug-Eluting Stents with Different Links on Hemodynamics and Drug Concentration Distribution. *J. Mech. Med. Biol.* **2013**, *13*, doi:10.1142/S021951941350070X.
210. Vijayaratnam, P.; Reizes, J.; Barber, T. The Impact of Strut Profile Geometry and Malapposition on the Haemodynamics and Drug-Transport Behaviour of Arteries Treated with Drug-Eluting Stents. *Int. J. Numer. METHODS HEAT FLUID FLOW* **2022**, *32*, 3881–3907, doi:10.1108/HFF-03-2022-0145.
211. Mandal, A.P.; Mandal, P.K. On the Role of Luminal Flow and Interstrut Distance in Modelling Drug Transport from Half-Embedded Drug-Eluting Stent. *Glob. J. Sci. Front. Res.* **2017**, *16*.

 doi:10.20944/preprints202606.0497.v1

212. Dong, R.; Jiang, W.; Yan, F.; Zheng, T.; Fan, Y. Numerical Analysis of the Impact of Atherosclerotic Plaque and Different Stent Spacing on Drug Deposition. *J. Mech. Med. Biol.* **2015**, *15*, doi:10.1142/S0219519415500116.
213. O'Connell, B.M.; Cunnane, E.M.; Denny, W.J.; Carroll, G.T.; Walsh, M.T. Improving Smooth Muscle Cell Exposure to Drugs from Drug-Eluting Stents at Early Time Points: A Variable Compression Approach. *Biomech. Model. Mechanobiol.* **2014**, *13*, 771–781, doi:10.1007/s10237-013-0533-9.
214. Leesar, M.; Feldman, M. Thrombosis and Myocardial Infarction: The Role of Bioresorbable Scaffolds. *J. Cardiovasc. AGING* **2023**, *3*, doi:10.20517/jca.2022.41.
215. Sakamoto, S.; Kawarada, O.; Kanaya, T.; Otsuka, F.; Harada, K.; Ogawa, H.; Yasuda, S. Vascular Response to Bare Metal Stents in the Superficial Femoral Artery as Assessed on Optical Coherence Tomography. *Circ. J. Off. J. Jpn. Circ. Soc.* **2015**, *79*, 441–443, doi:10.1253/circj.CJ-14-1069.
216. Scicolone, R.; Paraskevas, K.I.; Argiolas, G.; Balestrieri, A.; Siotto, P.; Suri, J.S.; Porcu, M.; Mantini, C.; Caulo, M.; Masala, S.; et al. Atherosclerotic Abdominal Aortic Aneurysms on Computed Tomography Angiography: A Narrative Review on Spectrum of Findings, Structured Reporting, Treatment, Secondary Complications and Differential Diagnosis. *Diagn. Basel Switz.* **2025**, *15*, doi:10.3390/diagnostics15060706.
217. Knuttinen, M.-G.; Naidu, S.; Oklu, R.; Kriegshauser, S.; Eversman, W.; Rotellini, L.; Thorpe, P.E. May-Thurner: Diagnosis and Endovascular Management. *Cardiovasc. Diagn. Ther.* **2017**, *7*, S159–S164, doi:10.21037/cdt.2017.10.14.
218. Silber, S.; Gutiérrez-Chico, J.L.; Behrens, S.; Witzenbichler, B.; Wiemer, M.; Hoffmann, S.; Slagboom, T.; Harald, D.; Suryapranata, H.; Nienaber, C.; et al. Effect of Paclitaxel Elution from Reservoirs with Bioabsorbable Polymer Compared to a Bare Metal Stent for the Elective Percutaneous Treatment of de Novo Coronary Stenosis: The EUROSTAR-II Randomised Clinical Trial. *EuroIntervention J. Eur. Collab. Work. Group Interv. Cardiol. Eur. Soc. Cardiol.* **2011**, *7*, 64–73, doi:10.4244/EIJV7I1A13.
219. Iqbal, J.; Gunn, J.; Serruys, P. Coronary Stents: Historical Development, Current Status and Future Directions. *Br. Med. Bull.* **2013**, *106*, 193–211, doi:10.1093/bmb/ldt009.
220. Nicolas, J.; Pivato, C.; Chiarito, M.; Beerkens, F.; Cao, D.; Mehran, R. Evolution of Drug-Eluting Coronary Stents: A Back-and-Forth Journey from the Bench to Bedside. *Cardiovasc. Res.* **2023**, *119*, 631–646, doi:10.1093/cvr/cvac105.
221. Sanz-Sánchez, J.; Chiarito, M.; Gill, G.S.; van der Heijden, L.C.; Piña, Y.; Cortese, B.; Alfonso, F.; von Birgelen, C.; Diez Gil, J.L.; Waksman, R.; et al. Small Vessel Coronary Artery Disease: Rationale for Standardized Definition and Critical Appraisal of the Literature. *J. Soc. Cardiovasc. Angiogr. Interv.* **2022**, *1*, 100403, doi:10.1016/j.jscai.2022.100403.
222. Jaramillo, S.; de Pontes, V.B.; Pinilla, J.A.; Stabile, F.; Felix, N.; Clemente, M.R.C.; Garot, P. Comparative Efficacy and Safety of Latest Generation Ultrathin and Thin Biodegradable Polymer vs. Durable Polymer Drug-Eluting Stents in Small Vessel Coronary Artery Disease: A Systematic Review and Meta-Analysis. *Cardiovasc. Revascularization Med. Mol. Interv.* **2025**, S1553-8389(25)00356-2, doi:10.1016/j.carrev.2025.07.004.
223. Boden, W.E.; De Caterina, R.; Kaski, J.C.; Bairey Merz, N.; Berry, C.; Marzilli, M.; Pepine, C.J.; Barbato, E.; Stefanini, G.; Prescott, E.; et al. Myocardial Ischemic Syndromes: A New Nomenclature to Harmonize Evolving International Clinical Practice Guidelines. *Circulation* **2024**, *150*, 1631–1637, doi:10.1161/CIRCULATIONAHA.123.065656.
224. Yang, H.; Seo, K.; Yoon, J.; Kim, H.; Chang, K.; Lim, H.; Choi, B.; Choi, S.; Yoon, M.; Lee, S.; et al. Clinical and Angiographic Outcomes of the First Korean-Made Sirolimus-Eluting Coronary Stent with Abluminal Bioresorbable Polymer. *KOREAN Circ. J.* **2017**, *47*, 898–906, doi:10.4070/kcj.2017.0094.
225. Arbab-Zadeh, A.; Graham, M.; Garcia-Garcia, H.M.; Mancini, G.J.; Weintraub, W.S.; Boden, W.E. Left Main Disease: The Last Frontier for Medical Therapy in Stable Coronary Artery Disease? *Eur. Cardiol.* **2025**, *20*, e24, doi:10.15420/ecr.2025.28.
226. Abdallah Mouin S.; Wang Kaijun; Magnuson Elizabeth A.; Osnabrugge Ruben L.; Kappetein A. Pieter; Morice Marie-Claude; Mohr Friedrich A.; Serruys Patrick W.; Cohen David J.; null null Quality of Life After Surgery or DES in Patients With 3-Vessel or Left Main Disease. *JACC* **2017**, *69*, 2039–2050, doi:10.1016/j.jacc.2017.02.031.

 doi:10.20944/preprints202606.0497.v1

227. Tudino, R.; Richardson, E.; Gonzalez, J.M.; Barghout, M.; Ho, T.; Abbott, J.D.; Saad, M. Acute Coronary-Occlusion Myocardial Infarctions: Performance of the STEMI Criteria and Evolving Alternative Approaches. *Trends Cardiovasc. Med.* **2025**, doi:10.1016/j.tcm.2025.10.006.
228. Buccheri, D.; Piraino, D.; Chirco, P.R.; Cortese, B. Performance of Bioresorbable Vascular Scaffolds versus Cobalt-Chromium Everolimus-Eluting Stent in Patients with ST-Elevation Myocardial Infarction Undergoing Primary Percutaneous Coronary Intervention: A Review of Currently Available Clinical Data. *Minerva Cardioangiol.* **2016**, *64*, 74–83.
229. Piuhola, J.; Holmström, L.T.A.; Niemelä, M.; Kervinen, K.; Tulppo, M.; Asikainen, R.; Hypèn, L.; Junttila, M.J. Three-Year Outcomes Related to Coronary Stenting; a Registry-Based Real-Life Population Study. *Scand. Cardiovasc. J. SCJ* **2020**, *54*, 162–168, doi:10.1080/14017431.2019.1693057.
230. Lin, C.-F.; Chang, Y.-H.; Yu, F.-C.; Tsai, C.-T.; Chen, C.-C.; Liu, H.-Y.; Chien, L.-N. Risk of Heart Failure Following Drug-Eluting Stent Implantation in Patients with Non-ST-Elevation Myocardial Infarction. *Atherosclerosis* **2021**, *316*, 84–89, doi:10.1016/j.atherosclerosis.2020.10.012.
231. Rha, S.W.; Choi, S.Y.; Choi, B.G.; Byun, J.K.; Cha, J.; Hyun, S.; Park, S.; Kim, J.B.; Choi, C.U. Ten-Year Major Clinical Outcomes between First- and Second-Generation Drug-Eluting Stents in Unstable Angina Patients Underwent Percutaneous Coronary Intervention. *Eur. Heart J.* **2023**, *44*, ehad655.1540, doi:10.1093/eurheartj/ehad655.1540.
232. Jaff, M.R.; White, C.J.; Hiatt, W.R.; Fowkes, G.R.; Dormandy, J.; Razavi, M.; Reekers, J.; Norgren, L. An Update on Methods for Revascularization and Expansion of the TASC Lesion Classification to Include Below-the-Knee Arteries: A Supplement to the Inter-Society Consensus for the Management of Peripheral Arterial Disease (TASC II): The TASC Steering Committee*. *Catheter. Cardiovasc. Interv.* **2015**, *86*, 611–625, doi:10.1002/ccd.26122.
233. Haghighat, L.; Altin, S.E.; Attaran, R.R.; Mena-Hurtado, C.; Regan, C.J. Review of the Latest Percutaneous Devices in Critical Limb Ischemia. *J. Clin. Med.* **2018**, *7*, doi:10.3390/jcm7040082.
234. Cui, H.-J.; Wu, Y.-F. Bioresorbable Scaffolds for Below-the-Knee Arterial Disease: A Literature Review of New Developments. *Rev. Cardiovasc. Med.* **2024**, *25*, 133, doi:10.31083/j.rcm2504133.
235. Ipema, J.; Kum, S.; Huizing, E.; Schreve, M.A.; Varcoe, R.L.; Hazenberg, C.E.; DE Vries, J.-P.; ÜnlÜ, Ç. A Systematic Review and Meta-Analysis of Bioresorbable Vascular Scaffolds for below-the-Knee Arterial Disease. *Int. Angiol. J. Int. Union Angiol.* **2021**, *40*, 42–51, doi:10.23736/S0392-9590.20.04462-4.
236. Kareem, A.K.; Gabir, M.M.; Ali, I.R.; Ismail, A.E.; Taib, I.; Darlis, N.; Almoayed, O.M. A Review on Femoropopliteal Arterial Deformation during Daily Lives and Nickel-Titanium Stent Properties. *J. Med. Eng. Technol.* **2022**, *46*, 300–317, doi:10.1080/03091902.2022.2041749.
237. Kim, J.; Ko, Y.-G.; Lee, S.-J.; Ahn, C.-M.; Rha, S.-W.; Choi, C.U.; Min, P.-K.; Park, J.K.; Jang, J.-Y.; Youn, Y.J.; et al. Korean Multicenter Registry of ELUVIA Stent for Femoropopliteal Artery Disease: K-ELUVIA Registry. *Korean Circ. J.* **2024**, *54*, 565–576, doi:10.4070/kcj.2024.0038.
238. Choi, W.; Rha, S.; Choi, B.; Park, S.; Kim, J.; Kang, D.; Choi, C.; Seo, Y.; Cho, Y.; Park, S.; et al. Balloon-Expandable Cobalt Chromium Stent versus Self-Expandable Nitinol Stent for the Atherosclerotic Iliac Arterial Disease (SENS-ILIAC Trial) Trial: A Randomized Controlled Trial. *HEART VESSELS* **2024**, *39*, 1060–1067, doi:10.1007/s00380-024-02431-4.
239. Brodmann, M.; Nemes, B.; Moreels, N.; Austermann, M.; Schmehl, J.; Robijn, J.; Rammos, C.; Müller-Hülsbeck, S.; Keirse, K.; Coscas, R.; et al. Dynetic-35 Cobalt Chromium Balloon-Expandable Stent for Iliac Lesions: 12-Month Results of the BIONETIC-I Multi-Center Study. *CVIR Endovasc.* **2025**, *8*, doi:10.1186/s42155-025-00633-z.
240. Buja, L.M.; Zhao, B.; Vela, D.; Segura, A.; Narula, N. Pathobiology of Aortic Aneurysms and Dissections: Synthesis of Recent Investigations and Evolving Insights. *JACC Adv.* **2025**, *4*, 101682, doi:10.1016/j.jacadv.2025.101682.
241. Sayed, A.; Munir, M.; Bahbah, E. Aortic Dissection: A Review of the Pathophysiology, Management and Prospective Advances. *Curr. Cardiol. Rev.* **2021**, *17*, doi:10.2174/1573403X16666201014142930.
242. Zarrintan, S.; Fallentine, J.; Yei, K.; Hamouda, M.; Ross, E.; Lee, J.; Malas, M. Real-World Outcomes of Open Surgical Repair vs Endovascular Aortic Repair in Ruptured Abdominal Aortic Aneurysms: Does Neck Anatomy Make a Difference? *J. Vasc. Surg.* **2025**, *86*.

 doi:10.20944/preprints202606.0497.v1

243. Guo, W.; Sun, G.; Zhang, H.; Xin, S.; Chen, Z.; Dai, X.; Fu, W.; Chang, G.; Zhang, H.; Li, Z.; et al. The G-Branch off-the-Shelf Mixed Branch Endograft for Thoracoabdominal Aortic Aneurysm: 1-Year Results from a Prospective Multicenter Study. *Int. J. Surg.* **2025**.
244. Malvindi, P.G.; Alfonsi, J.; Berretta, P.; Cefarelli, M.; Gatta, E.; Di Eusanio, M. Normothermic Frozen Elephant Trunk: Our Experience and Literature Review. *Cardiovasc. Diagn. Ther.* **2022**, *12*, 262–271, doi:10.21037/cdt-22-73.
245. Arita, Y.; Ishibashi, T.; Nakaoka, Y. Current Immunosuppressive Treatment for Takayasu Arteritis. *Circ. J.* **2024**, *88*, 1605–1609, doi:10.1253/circj.CJ-23-0780.
246. Hajiyev, K.; Forsting, M.; Cimpoca, A.; Khanafer, A.; Bäzner, H.; Henkes, H. Multiple Severe Intracranial Stenoses with Ischemic Stroke in Neuroborreliosis-Associated Cerebral Vasculitis: Endovascular Treatment Strategies and Literature Review. *Clin. Neuroradiol.* **2024**, *34*, 959–972, doi:10.1007/s00062-024-01447-7.
247. Chirico, C.; Giorgianni, A.; Clivio, V.; Malnati, S.; Gatta, T.; Vizzari, F.A.; Pellegrino, C.; Fusco, M.; Piacentino, F.; Venturini, M.; et al. Long-Term Successfully Endovascular Treatment of a Complicated Takayasu's Arteritis with Thrombectomy and Stenting: A Case Report. *J. Med. Case Reports* **2025**, *19*, 202, doi:10.1186/s13256-024-04989-z.
248. Schieferdecker, S.; Caspers, J.; Daniel, W.; Cornelius, J.F.; Muhammad, S. Surgical and Endovascular Cerebral Revascularization for Cerebral Vasculitis with Inflammatory Vessel Stenosis: A Case Series. *Acta Neurochir. (Wien)* **2024**, *166*, 103, doi:10.1007/s00701-024-06007-z.
249. Seinturier, C.; Thony, F.; Blaise, S.; Pernod, G.; Carpentier, P.H. Recanalization and Stenting of a Post-Thrombotic Iliac Vein in a Patient with Behçet's Disease. *J. Vasc. Surg. Venous Lymphat. Disord.* **2014**, *2*, 324–326, doi:10.1016/j.jvsv.2013.11.002.
250. Farina, R.; Foti, P.V.; Pennisi, I.; Vasile, T.; Clemenza, M.; Rosa, G.L.; Crimi, L.; Catalano, M.; Vacirca, F.; Basile, A. Vascular Compression Syndromes: A Pictorial Review. *Ultrason. Seoul Korea* **2022**, *41*, 444–461, doi:10.14366/usg.21233.
251. Bertino, F.J.; Hawkins, C.M.; Woods, G.M.; Shah, J.H.; Variyam, D.E.; Patel, K.N.; Gill, A.E. Technical Feasibility and Clinical Efficacy of Iliac Vein Stent Placement in Adolescents and Young Adults with May-Thurner Syndrome. *Cardiovasc. Intervent. Radiol.* **2024**, *47*, 45–59, doi:10.1007/s00270-023-03628-2.
252. Sarikaya, S.; Altas, O.; Ozgur, M.M.; Hancer, H.; Yilmaz, F.; Karagoz, A.; Ozer, T.; Aksut, M.; Ozen, Y.; Kirali, K. Treatment of Nutcracker Syndrome with Left Renal Vein Transposition and Endovascular Stenting. *Ann. Vasc. Surg.* **2024**, *102*, 110–120, doi:10.1016/j.avsg.2023.11.036.
253. Kilby, J.; Krishnaswamy, M.; George, S. Acute Bilateral External Iliac Artery Occlusion Following a Laparoscopic Incisional Hernia Repair. *BMJ Case Rep.* **2026**, *19*, e269992, doi:10.1136/bcr-2025-269992.
254. Rohit, M.K.; Gupta, A.; Khandelwal, N. Endovascular Transluminal Stent Grafting: Treatment of Choice for Post Lumbar Spine Surgery Iliac Arterio-Venous Fistulae. *Catheter. Cardiovasc. Interv. Off. J. Soc. Card. Angiogr. Interv.* **2016**, *88*, E203–E208, doi:10.1002/ccd.25245.
255. Gallerani, M.; Maida, G.; Boari, B.; Galeotti, R.; Rocca, T.; Gasbarro, V. High Output Heart Failure Due to an Iatrogenic Arterio-Venous Fistula after Lumbar Disc Surgery. *Acta Neurochir. (Wien)* **2007**, *149*, 1243–1247; discussion 1247, doi:10.1007/s00701-007-1397-5.
256. Jang, G.Y.; Ha, K.S. Self-Expandable Stents in Vascular Stenosis of Moderate to Large-Sized Vessels in Congenital Heart Disease: Early and Intermediate-Term Results. *Korean Circ. J.* **2019**, *49*, 932–942, doi:10.4070/kcj.2019.0067.
257. Khono, K.; Tamai, A.; Kobayashi, T.; Senzaki, H. Effects of Stent Implantation for Peripheral Pulmonary Artery Stenosis on Pulmonary Vascular Hemodynamics and Right Ventricular Function in a Patient with Repaired Tetralogy of Fallot. *Heart Vessels* **2011**, *26*, 672–676, doi:10.1007/s00380-011-0131-7.
258. Vijayvergiya, R.; Kaur, N.; Kasinadhuni, G.; Sharma, A.; Lal, A.; Sood, A. Endovascular Stenting with a Drug-Eluting Stent of Transplanted Renal Artery Stenosis in a Dual Kidney Transplanted Patient. *J. Vasc. Bras.* **2021**, *20*, e20210054, doi:10.1590/1677-5449.210054.
259. Huang, M.; Jiang, Z.; Zhu, K.; Guan, S.; Li, H.; Yang, Y.; Chen, G.; Shan, H. Long-term outcomes of hepatic artery stent placement for patients with hepatic artery stenosis after orthotopic liver transplantation. *Zhonghua Yi Xue Za Zhi* **2008**, *88*, 2175–2178.

 doi:10.20944/preprints202606.0497.v1

260. de Oliveira Leite, T.F.; Pazinato, L.V.; Nunes, T.F.; da Motta Leal Filho, J.M. Endovascular Management of Giant Common Iliac Artery Pseudoaneurysm after Complications in Simultaneous Pancreas-Kidney Transplant: A Case Report. *J. Med. Case Reports* **2021**, *15*, 329, doi:10.1186/s13256-021-02944-w.
261. Li, X.; Hou, X.; He, X.; Li, D.; Wang, J.; Chen, X.; Le, Q.; Liu, D.; Zhu, Y. Research on the Microstructure Evolution and Degradation Behavior of Biomedical Mg-Al-Mn-La Alloys Assisted by Machine Learning. *J. Alloys Compd.* **2026**, *1050*, 185599, doi:10.1016/j.jallcom.2025.185599.
262. R. E. Hammam; A. A. A. Solyman; M. H. Alsharif; P. Uthansakul; M. A. Deif Design of Biodegradable Mg Alloy for Abdominal Aortic Aneurysm Repair (AAAR) Using ANFIS Regression Model. *IEEE Access* **2022**, *10*, 28579–28589, doi:10.1109/ACCESS.2022.3155645.
263. Mishra, R.K.; Singh, S.S. Comprehensive Review of Biological Response, Alloy Design, Strengthening Mechanisms, Performance Evaluation, and Surface Modifications of Titanium Alloys for Biomedical Applications. *Multiscale Multidiscip. Model. Exp. Des.* **2024**, *8*, 67, doi:10.1007/s41939-024-00658-2.
264. Wu, C.; Xu, Y.; Fang, J.; Li, Q. Machine Learning in Biomaterials, Biomechanics/Mechanobiology, and Biofabrication: State of the Art and Perspective. *Arch. Comput. Methods Eng.* **2024**, *31*, 3699–3765, doi:10.1007/s11831-024-10100-y.
265. Menze, R.; Hesse, B.; Kusmierczuk, M.; Chen, D.; Weitkamp, T.; Bettink, S.; Scheller, B. Synchrotron Microtomography Reveals Insights into the Degradation Kinetics of Bio-Degradable Coronary Magnesium Scaffolds. *Bioact. Mater.* **2024**, *32*, 1–11, doi:10.1016/j.bioactmat.2023.09.008.
266. Zhang, Z.; Gao, J.; Wei, S.; Song, B.; Yao, Y.; Zheng, X.; Zhang, Y.; Zhang, L.; Li, Q.; Wu, J.; et al. Lattice-Inspired NiTi-Based Metamaterials with Widely Tunable Mechanical-Superelastic Synergy. *Virtual Phys. Prototyp.* **2025**, *20*, e2444572, doi:10.1080/17452759.2024.2444572.
267. Chandra Hasa, J.M.; Narayanan, P.; Pramanik, R.; Arockiarajan, A. Harnessing Machine Learning Algorithms for the Prediction and Optimization of Various Properties of Polylactic Acid in Biomedical Use: A Comprehensive Review. *Biomed. Mater. Bristol Engl.* **2025**, *20*, doi:10.1088/1748-605X/ada840.
268. Zhao, S.; Shi, Y.; Huang, C.; Li, X.; Lu, Y.; Wu, Y.; Li, Y.; Wang, L. Integrating Machine Learning into Additive Manufacturing of Metallic Biomaterials: A Comprehensive Review. *J. Funct. Biomater.* **2025**, *16*, doi:10.3390/jfb16030077.
269. Dinc, R.; Ardic, N. Bioinspired Coronary Stents: A Technological Perspective on Exosome-Mimetic Nanoengineering and Mini-Review of Existing Platforms. *Rev. Cardiovasc. Med.* **2025**, *26*, 42781, doi:10.31083/RCM42781.
270. Dinc, R. Artificial Intelligence in Drug-Coated Cardiovascular Devices: A Narrative Review. *Rev. Cardiovasc. Med.* **2025**, *26*, 40892, doi:10.31083/RCM40892.
271. Lee, J.; Gharaibeh, Y.; Dong, P.; Dallan, L.A.P.; Pereira, G.T.R.; Kim, J.N.; Hoori, A.; Gu, L.; Bezerra, H.G.; Cortese, B.; et al. Computational Analysis of Intravascular OCT Images for Future Clinical Support: A Comprehensive Review. *IEEE Rev. Biomed. Eng.* **2026**, *19*, 396–411, doi:10.1109/RBME.2025.3530244.
272. Bisighini, B.; Aguirre, M.; Biancolini, M.E.; Trovalusci, F.; Perrin, D.; Avril, S.; Pierrat, B. Machine Learning and Reduced Order Modelling for the Simulation of Braided Stent Deployment. *Front. Physiol.* **2023**, *14*, 1148540, doi:10.3389/fphys.2023.1148540.
273. Ghorbannia, A.; Tanade, C.; Yousef, A.; Khan, N.S.; Vardhan, M.; Chi, J.T.; Roychowdhury, S.; Das, A.; Leopold, J.A.; Chi, E.C.; et al. Simulation-Based Machine Learning for Real-Time Assessment of Side-Branch Hemodynamics in Coronary Bifurcation Lesions. *Int J High Perform Comput Appl* 2025, *39*, 678–691.
274. Kapoor, A.; Jepson, N.; Bressloff, N.W.; Loh, P.H.; Ray, T.; Beier, S. The Road to the Ideal Stent: A Review of Stent Design Optimisation Methods, Findings, and Opportunities. *Mater. Des.* **2024**, *237*, 112556, doi:10.1016/j.matdes.2023.112556.
275. Jiang, Y.; Nie, D.; Zhang, L.; Tang, X.; Li, H.; Li, L.; He, H.; Liu, Y.; Mao, W.; Xiong, Z.; et al. Construction and Validation of a Predictive Model for Postoperative Stent Occlusion in Patients Undergoing Iliac Vein Stenting Based on an Explainable Machine Learning Model. *Front. Surg.* **2025**, *12*, 1707615, doi:10.3389/fsurg.2025.1707615.
276. Zhao, W.; Huang, L.; Zhu, M.; Li, X.; Liu, X.; Zhang, W.; Shao, C.; Li, Y. Integrated CT-Derived Fractional Flow Reserve and Perivascular Fat Attenuation Index: A Multimodal Approach to Predict in-Stent Restenosis. *Front. Cardiovasc. Med.* **2025**, *12*, 1703044, doi:10.3389/fcvm.2025.1703044.

 doi:10.20944/preprints202606.0497.v1

277. Albertini, J.-N.; Derycke, L.; Millon, A.; Soler, R. Digital Twin and Artificial Intelligence Technologies for Predictive Planning of Endovascular Procedures. *Semin. Vasc. Surg.* **2024**, *37*, 306–313, doi:10.1053/j.semvascsurg.2024.07.002.